AFRL-RW-EG-TR-2019-087

Auto-Practicum on the Ignition and Growth Model

Douglas V. Nance

Air Force Research Laboratory
Munitions Directorate/Ordnance Division
Lethality, Vulnerability and Survivability Branch
(AFRL/RWML)
Eglin AFB, FL 32542-5910

July 2019

Final Report for period 1 Jan 2017 – 28 Feb 2017

AIR FORCE RESEARCH LABORATORY
MUNITIONS DIRECTORATE

■ Air Force Materiel Command ■ United States Air Force ■ Eglin Air Force Base, FL 32542

NOTICE AND SIGNATURE PAGE

Using Government drawings, specifications, or other data included in this document for any purpose other than Government procurement does not in any obligate the U.S. Government. The fact that the Government formulated or supplied the drawings, specifications, or other data does not license the holder or any other person or corporation, or convey any rights or permission to manufacture, use, or sell any patented invention that may relate to them.

This report was cleared for public release by the 96th Air Base Wing, Public Affairs Office, and is available to the general public, including foreign nationals. Copies may be obtained from the Defense Technical Information Center (DTIC) < http://www.dtic.mil/dtic/index/html>.

AFRL-RW-EG-TR-2019-087 HAS BEEN REVIEWED AND IS APPROVED FOR PUBLICATION IN ACCORDANCE WITH ASSIGNED DISTRIBUTION STATEMENT.

FOR THE DIRECTOR:

==Original Signed==

JOHN D. CORLEY, PhD
Ordnance Sciences Core
Technical Competency Lead
Ordnance Division

==Original Signed==

KIRK J. VANDEN, PhD
Technical Advisor
Lethality, Vulnerability and Survivability Branch

==Original Signed==

PEDRO LOPEZ-FERNANDEZ
Program Manager
Lethality, Vulnerability and Survivability Branch

This report is published in the interest of scientific and technical information exchange, and its publication does not constitute the Government's approval or disapproval of its ideas or findings.

This page intentionally left blank

REPORT DOCUMENTATION PAGE

Form Approved
OMB No. 0704-0188

1. REPORT DATE *(DD-MM-YYYY)*	2. REPORT TYPE	3. DATES COVERED *(From - To)*
1-07-2019	Final Report	1 Jan 2017 – 28 Feb 2017

4. TITLE AND SUBTITLE

Auto-Practicum on the Ignition and Growth Model

5a. CONTRACT NUMBER

5b. GRANT NUMBER

5c. PROGRAM ELEMENT NUMBER
62602F

6. AUTHOR(S)

Douglas V. Nance

5d. PROJECT NUMBER
25024504

5e. TASK NUMBER

5f. WORK UNIT NUMBER
W0TP

7. PERFORMING ORGANIZATION NAME(S) AND ADDRESS(ES)

Air Force Research Laboratory, Munitions Directorate
Ordnance Division
Lethality, Vulnerability, and Survivability Branch (AFRL/RWML)
Eglin AFB FL 32542-6810

8. PERFORMING ORGANIZATION REPORT NUMBER

AFRL-RW-EG-TR-2019-087

9. SPONSORING / MONITORING AGENCY NAME(S) AND ADDRESS(ES)

Air Force Research Laboratory, Munitions Directorate
Ordnance Division
Lethality, Vulnerability, and Survivability Branch (AFRL/RWML)
Eglin AFB FL 32542-6810
Technical Advisor: Kirk J. Vanden, PhD

10. SPONSOR/MONITOR'S ACRONYM(S)

11. SPONSOR/MONITOR'S REPORT

AFRL-RW-EG-TR-2019-087

12. DISTRIBUTION / AVAILABILITY STATEMENT

Distribution A: Approved for public release; distribution unlimited. Approval Confirmation 96W-2017-0089, dated 20 March 2017

13. SUPPLEMENTARY NOTES

14. ABSTRACT

This paper documents a series of mathematical manipulations of the equations of state for the Ignition and Growth Reactive Flow Model leading to the derivation of the detonation properties for explosives LX-17 and Nitromethane. Following the writings of Kapila *et al.*, these meanderings serve as a body of scratch work leading, in part, to lay the groundwork for the development of a new detonation physics computer code. Further to this end, the Harten-Lax-van Leer shock-capturing scheme is applied to solve the shock tube problem for the detonation products by using the Jones-Wilkins-Lee equation of state as an integral part of the reactive flow model.

15. SUBJECT TERMS

detonation, shock wave, ignition, HLLC, MUSCL, Hugoniot

16. SECURITY CLASSIFICATION OF:			17. LIMITATION OF ABSTRACT	18. NUMBER OF PAGES	19a. NAME OF RESPONSIBLE PERSON
a. REPORT	b. ABSTRACT	c. THIS PAGE			Pedro A. Lopez-Fernandez
UNCLASSIFIED	UNCLASSIFIED	UNCLASSIFIED	SAR	48	19b. TELEPHONE NUMBER *(include area code)*

Standard Form 298 (Rev. 8-98)
Prescribed by ANSI Std. Z39.18

This page intentionally left blank

Table of Contents

List of Figures

List of Tables

Preface

Some three miles south of my boyhood home lies Fort Fisher, a pastoral stretch of land situated between the Atlantic Ocean and Cape Fear River. In the old days, it was a quiet place inhabited most of the time only by the ghosts of history. There, by the sea, a monument was erected in memory of many of those spirits. A granite pillar topped by a bronze globe rises skyward from a concrete and brick foundation. A bronzed, clay eagle with ashen wings symbolically extended to the North and the South sits atop the globe maintaining an eternal watch over the Atlantic. The monument commemorates one of the final battles of the American Civil War, the second battle of Fort Fisher.

History records that the Confederacy suffered severe material shortages for the duration of the war. Ammunition, propellants and other war supplies such as black powder had to be procured from the Bahamas and sailed to the port of Wilmington, North Carolina. The route, particularly its terminal stage near the North Carolina coast was treacherous indeed. The Union Navy implemented an extensive blockade along miles of coastline forcing the Confederacy to build special ships designed to penetrate the blockade. This type of ship, the so-called *Blockade Runner* was designed to be a fast, maneuverable ship with a low profile. To avoid the Union's blockading warships, a blockade runner would run dangerously close to coastal shallows. Its low profile made it difficult to see when close to shore, especially at night. Effectively, a blockade runner could penetrate the blockade frontier at high speed and then skim along the coast in shallows where deep draft Union vessels could not go. Evading the shoals and moving sandbars, its Captain could guide it safely to port where it could unload its sorely needed Cargo.

Blockade runner Captains were a unique breed, iron-nerved and dedicated seamen. They combined the knowledge and characteristics of a blue water sea captain and a river pilot. There was even a story of one Captain who guided his vessel to safe harbor while suffering in the final stages of Typhoid Fever; he succumbed shortly after docking in Wilmington. Near the coast, the Captain had to know the sea bottom, just how much water was below the keel at any time. His ship was designed to be agile and quick; it was not designed for tensile strength. If the Captain ran his ship aground, it would, in all likelihood, be smashed into pieces or easily destroyed by Union Navy target practice. In the 1860s, life was lived close to the edge, so little quarter was given to a hapless foe. As a hedge, the Confederacy constructed Fort Fisher, a long range gun emplacement naturally protected by high sand dunes. A cannon shot has little effect on a big pile of sand; it just tends to go *poof*, and that is about all that happens. Hence, the fort was rather secure. Fort Fisher housed powerful artillery in multiple arrays such as Battery Buchanan, and it stored significant amounts of powder and shot in underground magazines. Union ships dared not stray into the range of her guns since they could be fired with lethal accuracy. The firepower of this installation was highly successful, and for this reason, it dawned on Union command that Fort Fisher had to be destroyed to interdict Confederate supply lines and hopefully end the war.

Ultimately, in 1865, Fort Fisher was overrun by a massive force consisting of thousands of Union soldiers and Marines. The fight was a bloody overture consisting of a hailstorm of musket balls, cannon fire and later degenerated into sword, bayonet and hand-to-hand combat. It was a perdition graphically captured by an artist whose painting shows Union forces overrunning the dunes and gun emplacements. In modern day reflectance, I am reminded of a scene in the 2004 film *Alien vs. Predator* where the infestation of hundreds of aliens swarm the ceremonial ziggurat overwhelming the smaller force of predators. One might wonder if the makers of the film drew inspiration for this scene from a battle such this say, Iwo Jima or Saipan. I cannot say for sure.

Nevertheless, when I was a boy, I heard that one could still find musket balls in the soil on the grounds of Fort Fisher. But from my point of view, the most interesting thing about the campaign against Fort Fisher is not the battle itself. What peaks my interest is an earlier attack made on the fort with the use of explosives.

When I wrote an undergraduate research paper at my *Alma Mater*, the University of North Carolina at Wilmington, I came to understand that Fort Fisher's magazines were designed for maximum powder storage. You see, back in the day, the safe storage of energetic materials was not a major concern. After all, a farmer could probably go down to the local general store and buy all the black powder (and maybe even Nitroglycerine) that he could afford. Both belligerent parties in the Civil War made good use of human intelligence, e.g., espionage, the Cloak and Dagger or just plain old eavesdropping down at the local watering hole. Still, it is a testament to the effectiveness of the Union intelligence network that Yankee spies learned of the Rebel (not the Star Wars type) magazine design. Ultimately, the Union Navy conceived of a plan to explode the magazines via *sympathetic detonation*, the use of one detonation to cause another.

In a roundabout way, we arrive at detonation, the subject of this paper. To that end, as a boy growing up in the Deep South, I was raised in a small coastal town with one grocery store, one drug store and the reception of exactly two analog television stations via TV antenna (what's that?). In short, there wasn't much to do; school was boring, and I lived for Saturday morning cartoons, comic books and firecrackers (and anything else involving fire or explosions). My Dad was a Jack-of-all-Trades; he grew up working on his grandparent's farm. He had only six years of school as was common in the day because of the rigors of farm life, but then his schooling was effective. He was quite literate and good at math (or ciphering, as Jethro Bodine used to say). My Dad could build anything and operate anything, including heavy equipment. I believe that he used to work in a quarry; that's where he learned about explosives. I asked Dad about "dynamite"; I knew nothing about it, but I was fascinated. Dad wasn't much of a talker, but he did say, "Oh yeah, you know; you can take that stuff; cut it up and throw it in the fire. It'll burn, but it won't blow up." So I asked Dad; well, what makes it blow up? He didn't really understand why himself, but he did reply, "Well, it takes a "jar" to make it blow up." What Dad was referring to is a shock wave.

Condensed explosives are most often detonated by the instantaneous, violent compression caused by the impact of shock wave on the explosive. Usually, this "jar" is administered by a detonator or "blasting cap". So back to the Civil War, the Union Navy's plan was to take a ship and load it to the gunwales with kegs of black powder. A system of synchronized mechanical clocks was designed to set off a multitude of fuses and ignite the confined powder. The ship would be parked offshore from Fort Fisher, and the clock system started. The coordinated blast was thought to be strong enough to shock-detonate the underground magazines and destroy Fort Fisher. In time, this plan was approved and launched; I recall, as a night time operation. The clocks ticked down to zero, and an orange light rose above the horizon lighting Fort Fisher like an artificial sun. The rebels rushed onto the parapets and stared in awe at the heavenly light. They were open-mouth-shocked by the eruption, but the magazines did not detonate. As it happened, the Union clock system failed to initiate a coordinated blast. There was a series of tremendous subsonic blasts, but a massive shock wave never formed. A Union officer on an observation ship exclaimed, "That was a fizzle." The plan failed.

The Union did not fully understand the nature of the powder, much less the criticality of the initiation scheme. This fault is completely understandable since there was a war on, and there

was relatively little research in the military application of explosives. Remarkably enough, this operation was, in some sense, successful, but only in the area of *Psychological Warfare.* The Confederate forces at Fort Fisher and at the Wilmington garrison were shocked and to an extent, demoralized by the attack. To fully understand why, one would have to have lived in their circumstances. They could not believe that the Union had so much black powder that they could afford to waste in this tactical misadventure. The Confederacy was strapped for basic resources; it was only a matter of time. They could not prevail, and it began to dawn upon them.

In the pages that follow, my endeavor is to discuss a complete model of explosive performance from a very elementary level. Ultimately, I want to show step by step how the properties of the detonation are connected to the thermodynamics of the explosive material as defined in the continuum framework. In my view, this approach is one way to understand and predict the behavior of any explosive material. Other views, such as those made from an atomistic (or microscale or quantum) level are equally encouraged and praised as a pathway to better understanding and enlightenment for this field of research.

Douglas V. Nance
February 2017

Acknowledgements

The author is grateful to Professor D. Scott Stewart (Retired) of the University of Illinois, Urbana-Champaign for a continuing and fruitful dialogue on the subject of detonation physics. This effort has been funded by the Munitions Directorate of the Air Force Research Laboratory, a commitment of steadfast support for which the author is sincerely appreciative.

Summary

This paper documents a series of mathematical manipulations of the equations of state for the Ignition and Growth Reactive Flow Model leading to the derivation of the detonation properties for explosives LX-17 and Nitromethane. Following the writings of Kapila *et al.*, these meanderings serve as a body of scratch work leading, in part, to lay the groundwork for the development of a new detonation physics computer code. Further to this end, the Harten-Lax-van Leer shock-capturing scheme is applied to solve the shock tube problem for the detonation products by using the Jones-Wilkins-Lee equation of state as an integral part of the reactive flow model.

1 INTRODUCTION

This manuscript concentrates on elementary calculations involving the Ignition and Growth (I & G) reactive flow model, a product of research conducted in the field of detonation physics by C.M. Tarver and others.[1] It is no exaggeration to say that I & G model stands as a cornerstone of this discipline in that it has served to inspire the development of other models. There are three components (or equations) for this model:

(a) A Jones-Wilkins-Lee (JWL) equation of state for the unreacted (condensed or solid) explosive material

(b) A JWL equation of state for the gaseous detonation products

(c) A reaction rate law cast in terms of a reaction progress variable that switches between the unreacted and detonation product equations of state

A final, but required, part of this model is the empirically obtained data needed by the algebraic relations mentioned above. Item (c) possesses terms that model the progress rate in both the ignition and growth phases of the detonation process. Issues associated with the reaction rate are not addressed by this work but are slated for inclusion in a future publication. Instead, items (a) and (b) are explored in detail below, particularly from the viewpoint of determining steady state detonation properties. The discussions that follow are vested in the processes of mathematical derivation and practical calculation. Other more expository aspects of this topic are not emphasized here. This paper closely follows the work of Kapila *et al.*, an excellent reference on this reactive flow model.[2] The intent of this manuscript is to provide some more of the detailed equations behind this reference and to apply them to study explosive materials with some level of thoroughness prior to simulating the detonation process. From this stance, the content of this work is definitely not new, but it is important for understanding the elementary dynamics of condensed explosives. Of course, we must admit that many other reactive flow models have been deployed throughout the explosives research community going back for decades. For the individual researcher, the model chosen for application depends upon personal tastes and experience.

2 TECHNICAL DEVELOPMENT

2.1 Properties of the Detonation

In this section of the manuscript, practical mathematics are presented for the I & G model. For reasons of elucidating steady state detonation properties, the equations of state are brought to the forefront of the discussion.

2.1.1 Equation of State for the Unreacted Explosive

The equation of state for the unreacted explosive is in JWL form, a variation of the Mie-Gruneisen equation of state.[3] As shown in Reference 2, terms indicated by tildes ~ have physical dimensions. Terms without tildes are dimensionless. The complete equation of state is written in the form of a system of equations, i.e.,

$$\tilde{E}_s(v_s) = \frac{\tilde{P}_s v_s}{\omega_s} - \tilde{F}_s(v_s) + \tilde{F}_s(1) \tag{2.1.1.1}$$

$$\tilde{P}_s(v_s) = \frac{\omega_s}{v_s}\left[\tilde{C}_s T_s + \tilde{G}_s(v_s) + \tilde{F}_s(v_s)\right] \tag{2.1.1.2}$$

Note that the term v_s is the local volume ratio for the unreacted explosive. Although the definition is not rigorous, the ratio can be defined as follows

$$v_s = \frac{\tilde{v}_s}{v_{s0}} \tag{2.1.1.3}$$

where $\tilde{v}_s$ is the local specific volume of the unreacted explosive while v_{s0} is the initial specific volume of the unreacted explosive. Note that $\tilde{P}_s$ and $\tilde{E}_s$ are the pressure and internal energy per unit volume, respectively. As one may suspect, $\tilde{T}_s$ is the absolute temperature of the unreacted explosive. The parameters ω_s and C_s are, respectively, a dimensionless, adiabatic gamma-like quantity and the dimensioned specific heat capacity for the condensed explosive.[4] Functions $\tilde{F}_s$ and $\tilde{G}_s$ are the dimensioned JWL function forms given by

$$\tilde{F}_s(v_s) = \tilde{A}_s\left(\frac{v_s}{\omega_s} - \frac{1}{R_{1s}}\right)\exp\left(-R_{1s}v_s\right) + \tilde{B}_s\left(\frac{v_s}{\omega_s} - \frac{1}{R_{2s}}\right)\exp\left(-R_{2s}v_s\right) \tag{2.1.1.4}$$

$$\tilde{G}_s(v_s) = \frac{\tilde{A}_s}{R_{1s}}\exp\left(-R_{1s}v_s\right) + \frac{\tilde{B}_s}{R_{2s}}\exp\left(-R_{2s}v_s\right) \tag{2.1.1.5}$$

Observe that in these JWL functions, physical dimensions are carried exclusively by $\tilde{A}_s$ and $\tilde{B}_s$. All of the other terms, e.g., R_{1s} and R_{2s}, in the equations are dimensionless quantities. For the sake of completeness, the initial density for the condensed explosive is denoted as ρ_{s0} where

$$\rho_{s0} = \frac{1}{v_{s0}} \tag{2.1.1.6}$$

In (2.1.1.1), the internal energy per unit volume may be written as

$$\tilde{E}_s(v_s) = \frac{\tilde{e}_s(v_s)}{\tilde{v}_{s0}} = \rho_{s0}\,\tilde{e}_s(v_s) \tag{2.1.1.7}$$

It follows that the general forms for (2.1.1.1) and (2.1.1.2) can be written as

$$\tilde{P}_s = \tilde{P}_s(v_s, \tilde{E}_s) \tag{2.1.1.8}$$

$$\tilde{P}_s = \tilde{P}_s(v_s, \tilde{T}_s) \tag{2.1.1.9}$$

2.1.2 Equation of State for the Detonation Products

The equation of state for the detonation products also utilizes the JWL formulas. In this case, the equation of state is expressed as the system

$$\tilde{E}_g(v_g) = \frac{\tilde{p}_g\, v_g}{\omega_g} - \tilde{F}_g(v_g) - \tilde{Q} \tag{2.1.2.1}$$

$$\tilde{p}_g = \frac{\omega_g}{v_g}\left[\tilde{C}_g\,\tilde{T}_g + \tilde{G}_g(v_g) + \tilde{F}_g(v_g)\right] \tag{2.1.2.2}$$

Observe that (2.1.2.1), the energy per unit volume for the detonation products is offset by the detonation energy $\tilde{Q}$. As in the previous section, the JWL functions are written as

$$\tilde{F}_g(v_g) = \tilde{A}_g\left(\frac{v_g}{\omega_g} - \frac{1}{R_{1g}}\right)\exp\left(-R_{1g}\,v_g\right) + \tilde{B}_g\left(\frac{v_g}{\omega_g} - \frac{1}{R_{2g}}\right)\exp\left(-R_{2g}\,v_g\right) \tag{2.1.2.3}$$

$$\tilde{G}_g(v_g) = \frac{\tilde{A}_g}{R_{1g}}\exp\left(-R_{1g}\,v_g\right) + \frac{\tilde{B}_g}{R_{2g}}\exp\left(-R_{2g}\,v_g\right) \tag{2.1.2.4}$$

Note that v_g is the dimensionless specific volume ratio for the gas phase, i.e.,

$$v_g = \frac{\tilde{v}_g}{v_{s0}} = \rho_{s0}\,\tilde{v}_g \tag{2.1.2.5}$$

A relation to specific internal energy is given as

$$\tilde{E}_g(v_g) = \frac{\tilde{e}_g(v_g)}{v_{s0}} = \rho_{s0}\,\tilde{e}_g(v_g) \tag{2.1.2.6}$$

In terms of dimensions, $\tilde{A}_g$, $\tilde{B}_g$ and $\tilde{Q}$ have units of pressure while $\tilde{C}_g$ has units of pressure divided by temperature. The general forms (2.1.8,9) remain valid for this case.

2.1.3 Reaction Rate Expression

The I & G model utilizes an ordinary differential equation for the reaction progress variable. Specifically,

$$\begin{aligned}\frac{d\lambda}{dt} = {} & \tilde{I}(1-\lambda)^b\left(\frac{1}{v}-1-a\right)^x H\left(\lambda_{ig,\max}-\lambda\right) \\ & + \tilde{G}_1(1-\lambda)^c\lambda^d\,\tilde{p}^y H\left(\lambda_{G1,\max}-\lambda\right) \\ & + \tilde{G}_2(1-\lambda)^e\lambda^g\,\tilde{p}^z H\left(\lambda-\lambda_{G2,\min}\right)\end{aligned} \tag{2.1.3.1}$$

The first term on the right hand side of (2.1.3.1) is the ignition term while the second and third terms represent reaction growth. Parameters $\tilde{I}$, $\tilde{G}_1$, $\tilde{G}_2$, *a*, *b*, *c*, *d*, *e*, *g*, *x*, *y*, *z*, $\lambda_{ig,\max}$, $\lambda_{G1,\max}$ and $\lambda_{G2,\min}$ require empirical determination for the explosive material and perhaps for the explosive configuration. *H* is the Heaviside function, i.e.,

$$H(\theta) = \begin{cases} 0 & \theta < 0 \\ 1 & \theta \geq 0 \end{cases} \tag{2.1.3.2}$$

For a more thorough discussion of the terms in the rate expression, consult Reference 2.

2.1.4 Mixture Relationships for the Equations of State

The primary mixture rule applies to (dimensioned) specific volume. The mixture specific volume is defined as

$$\tilde{v} = (1-\lambda)\tilde{v}_s + \lambda\tilde{v}_g \tag{2.1.4.1}$$

By dividing by v_{s0}, the dimensionless version is obtained, i.e.,

$$v = (1-\lambda)v_s + \lambda v_g \tag{2.1.4.2}$$

All of the quantities in (2.1.4.2) are positive, and we have that $0 \le \lambda \le 1$, so it may be concluded that

$$v \ge (1-\lambda)v_s \tag{2.1.4.3}$$

and

$$v \ge \lambda v_g \tag{2.1.4.4}$$

These expressions are important for generating mixture Hugoniot curves. A second, critical mixture rule applies to specific internal energy through the use of (2.1.7). The mixture specific energy is given as

$$\tilde{e}(v_s, v_g) = (1-\lambda)\tilde{e}_s(\tilde{p}_s, v_s) + \lambda \tilde{e}_g(\tilde{p}_g, v_g) \tag{2.1.4.5}$$

Observe that (2.1.4.5) contains both dimensioned and dimensionless quantities. By dropping the function arguments and substituting (2.1.1.7) and (2.1.2.6), we obtain

$$\tilde{e} = \tilde{v}_{s0}\left[(1-\lambda)\tilde{E}_s + \lambda \tilde{E}_g\right] \tag{2.1.4.6}$$

With the use of (2.1.1.1) and (2.1.2.1), the mixture specific energy becomes

$$\tilde{e} = \tilde{v}_{s0}\left[(1-\lambda)\left\{\frac{\tilde{p}_s v_s}{\omega_s} - \tilde{F}_s(v_s) + \tilde{F}_s(1)\right\} + \lambda\left\{\frac{\tilde{p}_g v_g}{\omega_g} - \tilde{F}_g(v_g) - \tilde{Q}\right\}\right] \tag{2.1.4.7}$$

By applying an assumption of pressure equilibrium, i.e., $\tilde{p} = \tilde{p}_s = \tilde{p}_g$, (2.1.4.7) becomes

$$\tilde{e} = \tilde{v}_{s0}\left[(1-\lambda)\left\{\frac{\tilde{p} v_s}{\omega_s} - \tilde{F}_s(v_s) + \tilde{F}_s(1)\right\} + \lambda\left\{\frac{\tilde{p} v_g}{\omega_g} - \tilde{F}_g(v_g) - \tilde{Q}\right\}\right] \tag{2.1.4.8}$$

an equation of state for mixture specific energy.

By solving (2.1.1.2) and (2.1.2.2) respectively for $\tilde{T}_s$ and $\tilde{T}_g$, one obtains

$$\tilde{T}_s = \left(\frac{v_s}{\tilde{C}_s \omega_s}\right)\tilde{p} - \frac{\tilde{G}_s(v_s)}{\tilde{C}_s} - \frac{\tilde{F}(v_s)}{\tilde{C}_s} \tag{2.1.4.9}$$

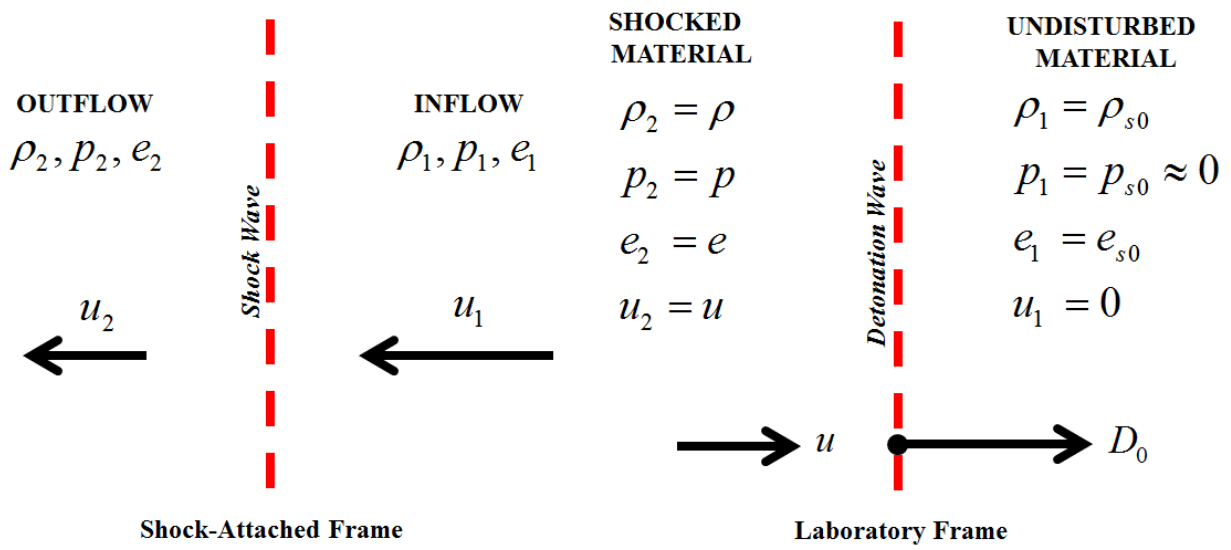

Figure 1. Detonation wave propagation in shock-attached and laboratory frames

$$\tilde{T}_g = \left(\frac{v_g}{\tilde{C}_g \omega_g}\right)\tilde{p} - \frac{\tilde{G}_g(v_g)}{\tilde{C}_g} - \frac{\tilde{F}(v_g)}{\tilde{C}_g} \tag{2.1.4.10}$$

At this point, temperature equilibrium ($\tilde{T} = \tilde{T}_s = \tilde{T}_g$) may be invoked; hence,

$$\left(\frac{v_s}{\tilde{C}_s \omega_s}\right)\tilde{p} - \frac{\tilde{G}_s(v_s)}{\tilde{C}_s} - \frac{\tilde{F}_s(v_s)}{\tilde{C}_s} = \left(\frac{v_g}{\tilde{C}_g \omega_g}\right)\tilde{p} - \frac{\tilde{G}_g(v_g)}{\tilde{C}_g} - \frac{\tilde{F}_g(v_g)}{\tilde{C}_g} \tag{2.1.4.11}$$

Rearrangement leads to a temperature equilibrium equation, i.e.,

$$\tilde{p}\left[\frac{v_s}{\tilde{C}_s \omega_s} - \frac{v_g}{\tilde{C}_g \omega_g}\right] - \frac{1}{\tilde{C}_s}\left[\tilde{F}_s(v_s) + \tilde{G}_s(v_s)\right] + \frac{1}{\tilde{C}_g}\left[\tilde{F}_g(v_g) + \tilde{G}(v_g)\right] = 0 \tag{2.1.4.12}$$

2.1.5 Governing Hydrodynamic Equations for Steady Detonation Solution

For performing an analysis of steady state detonation conditions, it is important to utilize the basic, hydrodynamic solution for the detonation problem.[4] This solution may be obtained with relative ease from an examination of the steady one-dimensional flow equations. Based upon the shock-attached frame shown in Figure 1, these equations are expressed as follows.

Mass Conservation:

$$\tilde{\rho}_2 \tilde{u}_2 = \tilde{\rho}_1 \tilde{u}_1 \tag{2.1.5.1}$$

Momentum Conservation:

$$\tilde{\rho}_2 \tilde{u}_2^2 + \tilde{p}_2 = \tilde{\rho}_1 \tilde{u}_1^2 + \tilde{p}_1 \tag{2.1.5.2}$$

Energy Conservation:

$$\tilde{e}_2 + \frac{\tilde{p}_2}{\tilde{\rho}_2} + \frac{1}{2}\tilde{u}_2^2 = \tilde{e}_1 + \frac{\tilde{p}_1}{\tilde{\rho}_1} + \frac{1}{2}\tilde{u}_1^2 \tag{2.1.5.3}$$

These equations are cast in the shock-attached frame for a plane shock wave. A steady, planar detonation wave can be analyzed by using these equations. The density, pressure, specific internal energy and velocity values can be assigned by using Figure 1 as a key for a steady detonation wave propagating at detonation velocity D_0 in laboratory (or steady) frame. Note that in the laboratory frame, *u* is particle velocity, the velocity of material at the outflow of the shock wave. In the shock attached frame, the corresponding velocity is

$$\tilde{u}_2 = \tilde{D}_0 - \tilde{u} \tag{2.1.5.4}$$

With the use of (2.1.5.4), (2.1.5.1) through (2.1.5.3) may be rewritten as

$$\tilde{\rho}\left(\tilde{D}_0 - \tilde{u}\right) = \tilde{\rho}_{s0}\tilde{D}_0 \tag{2.1.5.5}$$

$$\tilde{\rho}\left(\tilde{D}_0 - \tilde{u}\right)^2 + \tilde{p} = \tilde{\rho}_{s0}\tilde{D}_0^2 + \tilde{p}_{s0} \tag{2.1.5.6}$$

$$\tilde{e} + \frac{\tilde{p}}{\tilde{\rho}} + \frac{1}{2}\left(\tilde{D}_0 - \tilde{u}\right)^2 = \tilde{e}_{s0} + \frac{\tilde{p}_{s0}}{\tilde{\rho}_{s0}} + \frac{1}{2}\tilde{D}_0^2 \tag{2.1.5.7}$$

The subscript "s0" denotes quantities in the undisturbed material, i.e., the solid or condensed explosive material at the inflow of the detonation wave. By using the inverse relationship between density and specific volume, (2.1.5.5), (2.1.5.6) and (2.1.5.7) are rewritten as

$$\frac{\tilde{D}_0 - \tilde{u}}{\tilde{v}} = \frac{\tilde{D}_0}{\tilde{v}_{s0}} \tag{2.1.5.8}$$

$$\tilde{p} + \frac{\left(\tilde{D}_0 - \tilde{u}\right)^2}{\tilde{v}} = \tilde{p}_{s0} + \frac{\tilde{D}_0^2}{\tilde{v}_{s0}} \tag{2.1.5.9}$$

$$\tilde{e} + \tilde{p}\tilde{v} + \frac{1}{2}\left(\tilde{D}_0 - \tilde{u}\right)^2 = \tilde{e}_{s0} + \tilde{p}_{s0}\tilde{v}_{s0} + \frac{1}{2}\tilde{D}_0^2 \tag{2.1.5.10}$$

For detonation problems, the initial pressure of the undisturbed explosive is significantly lower than detonation pressure, so $\tilde{p}_{s0}$ is neglected. With this assumption and the substitution of (2.1.5.8), (2.1.5.9) becomes

$$\tilde{p} = \frac{\tilde{D}_0^2}{\tilde{v}_{s0}}\left(1 - \frac{\tilde{v}}{\tilde{v}_0}\right) = \frac{\tilde{D}_0^2}{\tilde{v}_{s0}}(1 - v) \tag{2.1.5.11}$$

This expression, cast in pressure and specific volume (or volume ratio), is identified as the Rayleigh line. Effectively, it is a line in the $\tilde{p} - v$ plane.

2.1.6 Single Phase Hugoniot Equations

In the way of review, a Hugoniot is a curve located in the equation of state surface. One of the most common manifestations of the Hugoniot is a $(\tilde{p}, \tilde{v})$ or $(\tilde{p}, v)$ curve that is the locus of shocked states consistent with the conservation equations (2.1.5.8-10), and of course, with the equation of state. By considering the equation for mixture specific energy (2.1.4.8), an entry point may be devised for the Hugoniot equation with the reaction progress variable λ as a parameter. Substitute (2.1.4.8) into (2.1.5.10), and we obtain

$$\tilde{v}_{s0}\left[(1-\lambda)\left\{\frac{\tilde{p}\,v_s}{\omega_s} - \tilde{F}_s(v_s) + \tilde{F}_s(1)\right\} + \lambda\left\{\frac{\tilde{p}\,v_g}{\omega_g} - \tilde{F}_g(v_g) - \tilde{Q}\right\}\right] + \tilde{p}\,\tilde{v} + \frac{1}{2}\left(\tilde{D}_0 - \tilde{u}\right)^2 = \tilde{e}_{s0} + \frac{1}{2}\tilde{D}_0^2 \tag{2.1.6.1}$$

A simplifying relation can be obtained from (2.5.8), i.e.,

$$\left(\tilde{D}_0 - \tilde{u}\right)^2 = \frac{\tilde{D}_0^2\,\tilde{v}^2}{v_{s0}^2} = \tilde{D}_0^2\,v^2 \tag{2.1.6.2}$$

This expression is substituted into (2.6.1) to obtain

$$(1-\lambda)\left\{\frac{\tilde{p}\,v_s}{\omega_s} - \tilde{F}_s(v_s) + \tilde{F}_s(1)\right\} + \lambda\left\{\frac{\tilde{p}\,v_g}{\omega_g} - \tilde{F}_g(v_g) - \tilde{Q}\right\} + \tilde{p}\,\frac{\tilde{v}}{\tilde{v}_{s0}} + \frac{1}{2}\frac{\tilde{D}_0^2}{\tilde{v}_{s0}}\left(v^2 - 1\right) = \frac{\tilde{e}_{s0}}{\tilde{v}_{s0}} \tag{2.1.6.3}$$

or

$$(1-\lambda)\left\{\frac{\tilde{p}\,v_s}{\omega_s} - \tilde{F}_s(v_s) + \tilde{F}_s(1)\right\} + \lambda\left\{\frac{\tilde{p}\,v_g}{\omega_g} - \tilde{F}_g(v_g) - \tilde{Q}\right\} + \tilde{p}\,v + \frac{1}{2}\frac{\tilde{D}_0^2}{\tilde{v}_{s0}}\left(v^2 - 1\right) = \frac{\tilde{e}_{s0}}{\tilde{v}_{s0}} \tag{2.1.6.4}$$

By simplifying with the use of (2.1.5.11), we obtain

$$(1-\lambda)\left\{\frac{\tilde{p}\,v_s}{\omega_s} - \tilde{F}_s(v_s) + \tilde{F}_s(1)\right\} + \lambda\left\{\frac{\tilde{p}\,v_g}{\omega_g} - \tilde{F}_g(v_g) - \tilde{Q}\right\} + \tilde{p}\,v - \frac{1}{2}\tilde{p}(1+v) = \frac{\tilde{e}_{s0}}{\tilde{v}_{s0}} \tag{2.1.6.5}$$

or

$$(1-\lambda)\left\{\frac{\tilde{p}v_s}{\omega_s}-\tilde{F}_s(v_s)+\tilde{F}_s(1)\right\}+\lambda\left\{\frac{\tilde{p}v_g}{\omega_g}-\tilde{F}_g(v_g)-\tilde{Q}\right\}+\frac{1}{2}\tilde{p}(v-1)=\frac{\tilde{e}_{s0}}{\tilde{v}_{s0}} \qquad (2.1.6.6)$$

This equation can be organized into forms containing a factor of pressure. One such form is

$$\tilde{p}\left[\frac{(1-\lambda)v_s}{\omega_s}+\frac{\lambda v_g}{\omega_g}+\frac{v-1}{2}\right]+(1-\lambda)\left[\tilde{F}_s(1)-\tilde{F}_s(v_s)\right]-\lambda\tilde{F}_g(v_g)=\lambda\tilde{Q} \qquad (2.1.6.7)$$

Since the road to it travels a wandering route, (2.1.6.7) deserves some discussion. This expression is produced by the simultaneous solution of the mixture equation for specific internal energy with the conservation of energy equation. This result is combined with the Rayleigh line formula, in itself, an expression that represents the momentum conservation equation. This procedure departs from the more standard approach of combining the conservation of energy and momentum equations to derive the so-called "Hugoniot Equation".[4,5] Typically, it is this relationship that is united with the equation of state to derive the actual Hugoniot (also called the Shock-Hugoniot) for the material in question. The process implied here accomplishes the same thing albeit with reordered mathematical operations. Unfortunately, (2.1.6.7) is not in true Hugoniot form (from a rigorous standpoint) since it relies upon $\tilde{p}$, v_s, v_g and v, where v is the mixture volume ratio defined by (2.1.4.2). For arbitrary values of λ $(0<\lambda<1)$, an implicit solution is required in order to determine the Hugoniot. This process is described a bit letter in this work. That having been said, Hugoniots for the condensed explosive and for the detonation products can be extracted from (2.1.6.7) with ease. Consider the Hugoniot for the unreacted material; in this case, $\lambda=0$. It follows, that $v=v_s$.

$$\tilde{p}\left[\frac{v}{\omega_s}+\frac{v-1}{2}\right]+\tilde{F}_s(1)-\tilde{F}_s(v_s)=0 \qquad (2.1.6.8)$$

or by collecting terms within the brackets,

$$\tilde{p}\left[v\left(\frac{2+\omega_s}{2\omega_s}\right)-\frac{1}{2}\right]+\tilde{F}_s(1)-\tilde{F}_s(v_s)=0 \qquad (2.1.6.9)$$

the unreacted Hugoniot is revealed. For the fully reacted gaseous phase, $\lambda=1$, and $v=v_g$; $v_s=0$. When substituted in (2.1.6.7), the following expression arises.

$$\tilde{p}\left[\frac{v}{\omega_g}+\frac{v-1}{2}\right]-\tilde{F}_g(v)=\tilde{Q} \qquad (2.1.6.10)$$

Simplification yields the Hugoniot for the detonation products, i.e.,

$$\tilde{p}\left[v\left(\frac{2+\omega_g}{2\omega_g} \right) - \frac{1}{2} \right] - \tilde{F}_g(v) = \tilde{Q} \tag{2.1.6.11}$$

Hugoniots (2.1.6.9) and (2.1.6.11) may be explicitly evaluated as functions of v, $v \in [0,1]$. It is interesting to observe that (2.1.6.10) and (2.1.6.11) intersect for a single value of v. In the context of detonation physics, this fact is pathological. If the detonation equations of state are properly structured, these Hugoniots should not intersect. The JWL equation of state is famously flawed, (we love to hate it), but still, it remains useful even if in a grandfatherly way. As it happens, the point of intersect between the detonation Hugoniots delineates a lower bound on v. The intersection point is determined by equating pressure between (2.1.6.9) and (2.1.6.11). Doing so defines the following function:

$$f_{Int}(v_{\text{int}}) = \left[\left(\frac{2+\omega_g}{2\omega_g} \right) v_{\text{int}} - \frac{1}{2} \right] \left(\tilde{F}_s(v_{\text{int}}) - \tilde{F}_s(v_{\text{int}}) \right) - \left[\left(\frac{2+\omega_s}{2\omega_s} \right) v_{\text{int}} - \frac{1}{2} \right] \left(\tilde{F}_g(v_{\text{int}}) + \tilde{Q} \right) \tag{2.1.6.12}$$

The non-trivial root of (2.1.6.12) is the minimum allowable volume ratio for the Hugoniots.

2.1.7 Mixture Hugoniot Relations

A mixture Hugoniot can be calculated for each value of the reaction progress variable λ, $\lambda \in [0,1]$, creating a family of curves. This development goes back to the time of von Neumann.[6] For complex equations of state like the JWL, the Hugoniot requires numerical evaluation. Again, (2.1.6.7) is the starting point along with the mixture volume ratio equation (2.1.4.2). Recall that there are five unknowns $(\tilde{p}, v, v_s, v_g, \lambda)$ in (2.1.6.7). With the inclusion of the mixture volume equation, we have two equations in these unknowns. A temperature equilibrium relation (2.1.4.12) is included in the system to constitute the third equation. Solving for pressure in (2.1.6.7) and (2.1.4.12), we obtain respectively,

$$\tilde{p} = \frac{\lambda\left(\tilde{F}_g(v_g) + \tilde{Q} \right) - (1-\lambda)\left(\tilde{F}_s(1) - \tilde{F}_s(v_s) \right)}{\frac{(1-\lambda)v_s}{\omega_s} + \frac{\lambda v_g}{\omega_g} + \frac{v-1}{2}} \tag{2.1.7.1}$$

$$\tilde{p} = \frac{\frac{1}{\tilde{C}_s}\left(\tilde{F}_s(v_s) + \tilde{G}_s(v_s) \right) - \frac{1}{\tilde{C}_g}\left(\tilde{F}_g(v_g) + \tilde{G}_g(v_g) \right)}{\frac{v_s}{\omega_s \tilde{C}_s} - \frac{v_g}{\omega_g \tilde{C}_g}} \tag{2.1.7.2}$$

By equating (2.1.7.1) and (2.1.7.2), pressure is eliminated from the Hugoniot system. The resulting equation is

$$f(v,v_g,v_s,\lambda)=\frac{\lambda\left(\tilde{\tilde{F}}_g(v_g)+\tilde{Q}\right)-(1-\lambda)\left(\tilde{\tilde{F}}_s(1)-\tilde{\tilde{F}}_s(v_s)\right)}{\frac{(1-\lambda)v_s}{\omega_s}+\frac{\lambda v_g}{\omega_g}+\frac{v-1}{2}} - \frac{\frac{1}{\tilde{\tilde{C}}_s}\left(\tilde{\tilde{F}}_s(v_s)+\tilde{\tilde{G}}_s(v_s)\right)-\frac{1}{\tilde{\tilde{C}}_g}\left(\tilde{\tilde{F}}_g(v_g)+\tilde{\tilde{G}}_g(v_g)\right)}{\frac{v_s}{\omega_s\tilde{\tilde{C}}_s}-\frac{v_g}{\omega_g\tilde{\tilde{C}}_g}} \tag{2.1.7.3}$$

This result suggests a method for computing a mixture Hugoniot for a particular value of λ. For a choice of λ, calculations of (2.1.7.3) can be conducted for a sequence of v_i, $i=1,\ldots,n$ where $v_i\in(v_{\text{int}},1)$. Recall that v_{int} is given by solution of (2.1.6.12). Upon the selection of v_i, a finite sequence v_{sj} , $j=1,\ldots,m$ is defined; for example, we may choose $v_{s1}\approx 0.3$ and $v_{sm}=1.0$. For each v_{sj}, a consistent value of v_g is calculated as

$$v_g=\frac{v_i-(1-\lambda)v_{sj}}{\lambda} \tag{2.1.7.4}$$

With the guidance written in the paragraph above and with the use of (2.1.7.3), we have specified an ordered quadruple (v, v_s, v_g, λ). The function (2.1.7.3) is evaluated for this quadruple generated in the loop over v_{sj}. As the loop over these values, a change in the sign of f signifies the presence of a root. Hence, the point (v, v_s, v_g, λ) lies on the Hugoniot for λ. This result motivates the following algorithm.

Algorithm 2.1.7 – Calculating a Mixture Hugoniot

1. Determine the point of intersection between the two single phase detonation Hugoniots, i.e., solve (2.1.6.12) for v_{int}.

2. Select a value of λ to specify the mixture Hugoniot of interest.

3.Set the domain of volume ratio v in $[v_{\text{int}},1]$ as a discrete sequence v_i, $i=1,\ldots,n$ for a choice of *n*, the desired number of volume ratio points.

4. Loop over the v_i.

4a. Set the domain of v_s in $[\sim 0.3,1]$ as a discrete sequence v_{sj}, $j=1,\ldots,m$ for a choice of *m*.

4b. Loop over the v_{sj}.

4b-1. Compute v_g via (2.1.7.4).

4b-2. Construct the ordered quadruple (v_i, v_{sj}, v_g, λ).

4b-3. Evaluate $f(v_i,\ v_{sj},\ v_g,\ \lambda)$ via (2.1.7.3) and determine its sign.

4b-4. **If** the sign of *f* changes, an approximate root has been located. Refine the value v_{sj} by any desired means and compute the corresponding v_g. Verify that this new ordered quadruple satisfies $f(v_i,\ v_{sj},\ v_g,\ \lambda) = 0$. The resulting ordered quadruple $(v_i,\ v_{sj},\ v_g,\ \lambda)$ is a point on the Hugoniot.

Else, no root is detected. Increment *j* and continue with loop 4b.

2.1.8 Resolution of the Chapman-Jouquet State

The Chapman-Jouquet (CJ) state exists at the point of tangent intersection between the detonation products Hugoniot and the Rayleigh line. We recall that these formulas are respectively (from 2.6.11 and 2.5.11),

$$\tilde{p}\left[\left(\frac{2+\omega_g}{2\omega_g}\right)v-\frac{1}{2}\right]-\tilde{F}_g(v)=\tilde{Q} \tag{2.1.8.1}$$

$$\tilde{p}=\frac{\tilde{D}_0^2}{\tilde{v}_{s0}}(1-v) \tag{2.1.8.2}$$

According to the core reference (Kapila *et al.* [2]), applied for these notes, the CJ derivation begins with substitution of (2.8.1) into (2.8.2) eliminating $\tilde{p}$. Simplification yields

$$v^2-2\left(\frac{1+\omega_g}{2+\omega_g}\right)v+\frac{\omega_g}{2+\omega_g}+\left(\frac{2\omega_g}{2+\omega_g}\right)\frac{\tilde{v}_{s0}}{\tilde{D}_0^2}\left[\tilde{F}_g(v)+\tilde{Q}\right]=0 \tag{2.1.8.3}$$

This equation is now cast in terms of the two unknowns v and $\tilde{D}_0$, so a second equation is required to form a solvable system. In Reference 2, a second linearly independent equation is obtained by differentiating (2.1.8.3) with respect to v. Omitting the details, we simply provide the result.

$$2v-2\left(\frac{1+\omega_g}{2+\omega_g}\right)+\left(\frac{2\omega_g}{2+\omega_g}\right)\frac{\tilde{v}_{s0}}{\tilde{D}_0^2}\tilde{F}_g'(v)=0 \tag{2.1.8.4}$$

where, as a general form,

$$\tilde{F}_g'(v)=A_g\left[1+\frac{1}{\omega_g}+\frac{R_{1g}v}{\omega_g}\right]\exp\left(-R_{1g}v\right)+B_g\left[1+\frac{1}{\omega_g}+\frac{R_{2g}v}{\omega_g}\right]\exp\left(-R_{2g}v\right) \tag{2.1.8.5}$$

According to the reference, the root of (2.1.8.3) identifies the CJ volume ratio. Moreover, it is asserted that the root is in fact a double root. The parameter $\tilde{D}_o^2$ is eliminated by the simultaneous solution of (2.1.8.3) and (2.1.8.4). Again, the details are omitted, and the result is simply provided.

$$\tilde{F}_g'(v_{CJ}) - \left[\tilde{Q} + \tilde{F}_g(v_{CJ})\right]\left(\frac{1}{v_{CJ}-1} + \frac{1}{v_{CJ} - \dfrac{\omega_g}{2+\omega_g}}\right) = 0 \tag{2.1.8.6}$$

This method certainly works well, but we want and we pine for genuine physical insight. For this reason, an alternative derivation of the CJ state is provided below. The CJ state is defined as the point of tangency between the detonation products Hugoniot and the Rayleigh line. There are two technical requirements necessary to locate this point. The first requirement is to determine a common point $\left(v, \tilde{D}_0\right)$ between the detonation products Hugoniot and the Rayleigh line, i.e.,

$$\tilde{p}_{Hugo}(v, \tilde{D}_0) = \tilde{p}_{Rayleigh}(v, \tilde{D}_0) \tag{2.1.8.7}$$

By applying (2.1.8.7), (2.1.8.1) and (2.1.8.2) may be easily combined to derive the explicit expression

$$\frac{\tilde{D}_0^2}{v_{s0}}(1-v) = \frac{\tilde{F}_g(v) + \tilde{Q}}{\beta v - 1/2} \tag{2.1.8.8}$$

where

$$\beta = \frac{2+\omega_g}{2\omega_g} \tag{2.1.8.9}$$

The second technical requirement for the CJ point is the tangency condition between the Hugoniot and the Rayleigh line, i.e.,

$$\frac{d\,\tilde{p}_{Hugo}}{dv}\left(v, \tilde{D}_0\right) = \frac{d\,\tilde{p}_{Rayleigh}}{dv}\left(v, \tilde{D}_0\right) \tag{2.1.8.10}$$

Explicit forms needed by (2.1.8.10) may be derived. By differentiating (2.1.8.1), we obtain

$$\frac{d\,\tilde{p}_{Hugo}}{dv}(v, \tilde{D}_0) = \frac{(\beta v - 1/2)\tilde{F}_g'(v) - \left(\tilde{F}_g(v) + \tilde{Q}\right)\beta}{(\beta v - 1/2)^2} \tag{2.1.8.11}$$

Similarly, the derivative of (2.1.8.2) is computed as

$$\frac{d\,\tilde{p}_{Rayleigh}}{dv}\left(v,\tilde{D}_0\right)=-\frac{\tilde{D}_0^2}{\tilde{v}_{s0}} \tag{2.1.8.12}$$

By substituting (2.1.8.11) and (2.1.8.12) into (2.1.8.10), the tangency condition is expressed as

$$\frac{(\beta v-1/2)\tilde{F}_g'(v)-\left(\tilde{F}_g(v)+\tilde{Q}\right)\beta}{(\beta v-1/2)^2}=-\frac{\tilde{D}_0^2}{\tilde{v}_{s0}} \tag{2.1.8.13}$$

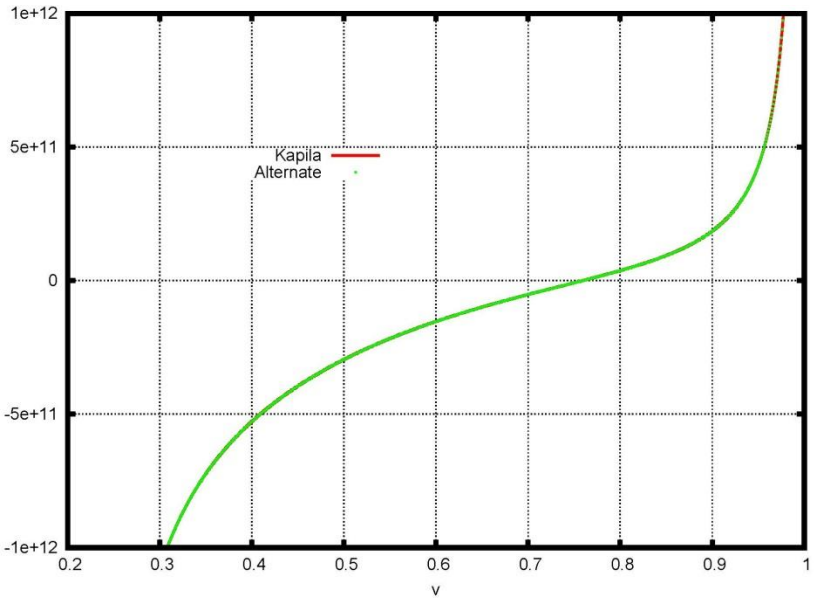

Figure 2. Comparison of CJ volume ratio equations (2.8.5) and (2.8.15)

If $\tilde{D}_0^2/\tilde{v}_{s0}$ is eliminated from (2.1.8.7) and (2.1.8.13), a result is that

$$\frac{(\beta v-1/2)\tilde{F}_g'(v)-\left(\tilde{F}_g(v)+\tilde{Q}\right)\beta}{(\beta v-1/2)^2}=-\frac{\tilde{F}_g(v)+\tilde{Q}}{(1-v)(\beta v-1/2)} \tag{2.1.8.14}$$

This expression can be simplified into a final form as

$$\tilde{F}_g'(v_{CJ})+\frac{[2\beta v_{CJ}-(\beta+1/2)]\left(\tilde{F}_g(v_{CJ})+\tilde{Q}\right)}{(1-v)(\beta v_{CJ}-1/2)}=0 \tag{2.1.8.15}$$

Equation (2.1.8.15) is the counterpart to (2.1.8.5), and the CL volume ratio is a root of (2.1.8.15). The advantage of the alternate derivation is that it clearly enforces both intrinsic properties of the CJ point. As is indicated by Figure 2, numerical experimentation indicates that these two different formulations are basically equivalent over the volume ratio range. Once that v_{CJ} is determined as the root of either of the two equations, CJ pressure is calculated from (2.1.8.1). Similarly, the detonation velocity is computed from the Rayleigh line formula (2.1.8.2), i.e.,

$$\tilde{D}_0 = \sqrt{\frac{\tilde{p}_{CJ}\,\tilde{v}_{s0}}{1-v_{CJ}}} \tag{2.1.8.16}$$

The particle velocity at the shock wave outflow is denoted $\tilde{u}_{CJ}$ and given by a rearrangement of (2.1.5.8), i.e.,

$$\tilde{u}_{CJ} = \tilde{D}_0(1-v_{CJ}) \tag{2.1.8.17}$$

2.1.9 Resolution of the von Neumann Spike

As in the preceding sections, Reference 2 is central to the discussion below. However, there is a small difference in lexicography applied here. The von Neumann (VN) spike is the sharp rise in pressure exhibited when the detonation wave strikes the solid explosive. Mathematically, this state exists on the Hugoniot for the unreacted explosive at the point of intersection with the Rayleigh line. In Reference 2, this point is referred to as the state behind the lead shock. The volume ratio at this point is derived through the simultaneous solution of the condensed phase Hugoniot and the Rayleigh line. Substitute (2.1.5.11) into (2.1.6.9) to begin the derivation.

$$\frac{\tilde{D}_0^2}{\tilde{v}_{s0}}(1-v)\left[v\left(\frac{2+\omega_s}{2\omega_s}\right)-\frac{1}{2}\right]+\tilde{F}_s(1)-\tilde{F}_s(v)=0 \tag{2.1.9.1}$$

Simplifying, we obtain

$$(1-v)\left[v\left(\frac{2+\omega_s}{2\omega_s}\right)-\frac{1}{2}\right]+\frac{\tilde{v}_{s0}}{\tilde{D}_0^2}\left(\tilde{F}_s(1)-\tilde{F}_s(v)\right)=0 \tag{2.1.9.2}$$

Factor out the term $(2+\omega_s)/(2\omega_s)$ and expand the binomial product on the left.

$$v-\frac{1}{2}\left(\frac{2\omega_s}{2+\omega_s}\right)-v^2+\left(\frac{2\omega_s}{2+\omega_s}\right)\frac{v}{2}+\left(\frac{2\omega_s}{2+\omega_s}\right)\frac{\tilde{v}_{s0}}{\tilde{D}_0^2}\left(\tilde{F}_s(1)-\tilde{F}_s(v)\right)=0 \tag{2.1.9.3}$$

By rearranging, we obtain the formula

$$v^2-2\left(\frac{1+\omega_s}{2+\omega_s}\right)v+\frac{\omega_s}{2+\omega_s}-\left(\frac{2\omega_s}{2+\omega_s}\right)\frac{\tilde{v}_{s0}}{\tilde{D}_0^2}\left(\tilde{F}_s(1)-\tilde{F}_s(v)\right)=0 \tag{2.1.9.4}$$

Note that $v=1$ is a root of (2.9.4) and represents the unshocked explosive. A second root, $v=v_{VN}$, the non-trivial root, describes the volume ratio corresponding to the von Neumann spike. Of course, (2.1.9.4) numerical solution is required in order to determine v_{VN}.

2.1.10 Scaling and the Removal of Physical Dimensions

Problems in both gas dynamics and detonation physics problems are characterized by physical properties with extreme variations in magnitude. Pressure and temperature are two exemplary properties in this regard. As is consistent with the structure of the reactive Euler equations, all of the associated properties can be consistently scaled for the removal of dimensions. The scaling factor for a particular property is designated by a subscript "*ref*". To provide the basic scaling factors, we follow Kapila *et. al.*[2]

Specific Volume:	$\tilde{v}_{ref} = \tilde{v}_{s0}$	Velocity:	$\tilde{u}_{ref} = \tilde{D}_0$
Pressure:	$\tilde{p}_{ref} = \tilde{D}_0^2 / \tilde{v}_{s0}$	Specific Energy:	$\tilde{e}_{ref} = \tilde{D}_0^2$
Temperature:	$\tilde{T}_{ref} = \tilde{T}_{s0}$	Time:	τ_{ref} (user's choice)
Length:	$\tilde{L}_{ref} = \tilde{\tau}_{ref} \tilde{D}_0$	Specific Heat:	$\tilde{C}_{ref} = \tilde{p}_{ref} / \tilde{T}_{ref}$
Reaction Rate:	$\tilde{R}_{ref} = 1/\tilde{\tau}_{ref}$		

Note that $\tilde{e}_{ref} = \tilde{p}_{ref} \tilde{v}_{s0} = \tilde{p}_{ref} \tilde{v}_{ref}$. This relationship is important for the non-dimensionalization of the JWL functions. Here, quantities marked by a tilde "~" possess dimensions. Remember; dimensions are general physical properties like length, mass, speed or electrical charge. Units are the corresponding specific quantities used to measure dimensions, e.g., meters, slugs, miles per hour or Coulombs. Quantities without the tilde notation are dimensionless; think pure numbers. Hence,

$$\begin{aligned}
&\tilde{x} = L_{ref}\, x && \tilde{y} = L_{ref}\, y && \tilde{z} = L_{ref}\, z \\
&\tilde{u} = u_{ref}\, u && \tilde{\upsilon} = u_{ref}\, \upsilon && \tilde{w} = u_{ref}\, w \\
&\tilde{p} = p_{ref}\, p && \tilde{\rho} = \rho_{ref}\, \rho && \tilde{T} = T_{ref}\, T \\
&\tilde{t} = \tau_{ref}\, t && \tilde{C} = C_{ref}\, C && \tilde{R} = R_{ref}\, R
\end{aligned} \qquad (2.1.10.1)$$

The scheme (2.1.10.1) presents a completely consistent system for removing dimensions from the equations used in this model. Removing dimensions from the governing reactive Euler equations is an easy exercise, so the result is simply stated below.

$$\frac{\partial \rho}{\partial t} + \frac{\partial (\rho u)}{\partial x} + \frac{\partial (\rho v)}{\partial y} + \frac{\partial (\rho w)}{\partial z} = 0 \qquad (2.1.10.2)$$

$$\frac{\partial (\rho u)}{\partial t} + \frac{\partial \left(\rho u^2 + P\right)}{\partial x} + \frac{\partial (\rho u v)}{\partial y} + \frac{\partial (\rho u w)}{\partial z} = 0 \qquad (2.1.10.3)$$

$$\frac{\partial (\rho v)}{\partial t} + \frac{\partial (\rho v u)}{\partial x} + \frac{\partial \left(\rho v^2 + P\right)}{\partial y} + \frac{\partial (\rho v w)}{\partial z} = 0 \qquad (2.1.10.4)$$

$$\frac{\partial(\rho w)}{\partial t}+\frac{\partial(\rho wu)}{\partial x}+\frac{\partial(\rho wv)}{\partial y}+\frac{\partial\left(\rho w^2+P\right)}{\partial z}=0 \tag{2.1.10.5}$$

$$\frac{\partial(\rho \varepsilon)}{\partial t}+\frac{\partial(\rho uH)}{\partial x}+\frac{\partial(\rho vH)}{\partial y}+\frac{\partial(\rho wH)}{\partial z}=0 \tag{2.1.10.6}$$

$$\frac{\partial(\rho \lambda)}{\partial t}+\frac{\partial(\rho u\lambda)}{\partial x}+\frac{\partial(\rho v\lambda)}{\partial y}+\frac{\partial(\rho w\lambda)}{\partial z}=\rho R \tag{2.1.10.7}$$

where the total energy per unit mass is

$$\varepsilon = e+\frac{1}{2}\left(u^2+v^2+w^2\right) \tag{2.1.10.8}$$

and the total enthalpy per unit mass is

$$H=\varepsilon+\frac{p}{\rho} \tag{2.1.10.9}$$

Consider the pressure-energy-volume relation for the solid material described by (2.1.1.1) and (2.1.1.7), i.e.,

$$\tilde{\tilde{E}}_s=\frac{\tilde{\tilde{e}}_s}{\tilde{\tilde{v}}_{s0}}=\frac{\tilde{\tilde{p}}\,v_s}{\omega_s}+\tilde{\tilde{F}}_s(1)-\tilde{\tilde{F}}_s(v_s) \tag{2.1.10.10}$$

Hence,

$$\tilde{\tilde{e}}_s=\tilde{\tilde{v}}_{s0}\left[\frac{\tilde{\tilde{p}}\,v_s}{\omega_s}+\tilde{\tilde{F}}_s(1)-\tilde{\tilde{F}}_s(v_s)\right] \tag{2.1.10.11}$$

Rules for non-dimensionalization can be applied to this equation as follows.

$$e_s\,e_{ref}=\tilde{\tilde{v}}_{s0}\left[\frac{p_{ref}\,p\,v_s}{\omega_s}+p_{ref}\,F_s(1)-p_{ref}\,F_s(v_s)\right] \tag{2.1.10.12}$$

Simplifying,

$$e_s(e_{ref})=(\tilde{\tilde{v}}_{s0}p_{ref})\left[\frac{p\,v_s}{\omega_s}+F_s(1)-F_s(v_s)\right] \tag{2.1.10.13}$$

Using the dimensional equivalence derived above, we obtain the $e_s=e_s(p,v_s)$ limb of the equation of state.

$$e_s=\frac{p\,v_s}{\omega_s}+F_s(1)-F_s(v_s) \tag{2.1.10.14}$$

On the other hand, consider the $\tilde{p}_s = \tilde{p}_s(v_s, \tilde{T}_s)$ limb of the condensed explosive equation of state. (Note that a similar analysis can be applied for the detonation product equation of state). Recalling (2.1.1.2),

$$\tilde{p}_s = \frac{\omega_s}{v_s}\left[\tilde{C}_s \tilde{T}_s + \tilde{G}_s(v_s) + \tilde{F}_s(v_s)\right] \tag{2.1.10.15}$$

Migrating terms into dimensionless form,

$$p_s \tilde{p}_{ref} = \frac{\omega_s}{v_s}\left[C_s \tilde{C}_{ref} T_s \tilde{T}_{ref} + G_s(v_s)\, \tilde{p}_{ref} + F_s(v_s)\tilde{p}_{ref}\right] \tag{2.1.10.16}$$

Substituting for the dimensional group $\tilde{C}_{ref}$,

$$p_s \tilde{p}_{ref} = \frac{\omega_s}{v_s}\left[C_s\left(\frac{\tilde{p}_{ref}}{\tilde{T}_{ref}}\right) T_s \tilde{T}_{ref} + G_s(v_s)\, \tilde{p}_{ref} + F_s(v_s)\tilde{p}_{ref}\right] \tag{2.1.10.17}$$

Thus,

$$p_s = \frac{\omega_s}{v_s}\left[C_s T_s + G_s(v_s) + F_s(v_s)\right] \tag{2.1.10.17}$$

is the dimensionless $p_s = p_s(v_s, T_s)$ limb of the condensed phase equation of state.

Also, it is important to consider the application of dimensional arguments to the JWL functions. Consider first the function F_s for the solid explosive although the same arguments can be applied to the detonation products equation of state. Recall that

$$\tilde{F}_s(v_s) = \tilde{A}_s\left(\frac{v_s}{\omega_s} - \frac{1}{R_{1s}}\right)\exp\left(-R_{1s}\, v_s\right) + \tilde{B}_s\left(\frac{v_s}{\omega_s} - \frac{1}{R_{2s}}\right)\exp\left(-R_{2s}\, v_s\right) \tag{2.1.10.18}$$

By examining (2.1.10.18), we observe that the dimensions are carried by coefficients $\tilde{A}_s$ and $\tilde{B}_s$. The remaining parameters v_s, R_{1s}, R_{2s} and ω_s are already dimension-free, so

$$\tilde{p}_{ref}\, F_s(v) = \tilde{p}_{ref} A_s\left(\frac{v_s}{\omega_s} - \frac{1}{R_{1s}}\right)\exp\left(-R_{1s} v_s\right) + \tilde{p}_{ref} B_s\left(\frac{v_s}{\omega_s} - \frac{1}{R_{2s}}\right)\exp\left(-R_{2s} v_s\right) \tag{2.1.10.19}$$

Factoring out $\tilde{p}_{ref}$, we obtain the dimensionless form

$$F_s(v_s) = A_s\left(\frac{v_s}{\omega_s} - \frac{1}{R_{1s}}\right)\exp\left(-R_{1s}v_s\right) + B_s\left(\frac{v_s}{\omega_s} - \frac{1}{R_{2s}}\right)\exp\left(-R_{2s}v_s\right) \qquad (2.1.10.20)$$

JWL function $\tilde{\tilde{G}}_s$ can be addressed in the same way. Recall that

$$\tilde{\tilde{G}}_s(v_s) = \frac{\tilde{\tilde{A}}_s}{R_{1s}}\exp\left(-R_{1s}\,v_s\right) + \frac{\tilde{\tilde{B}}_s}{R_{2s}}\exp\left(-R_{2s}\,v_s\right) \qquad (2.1.10.21)$$

Coefficients $\tilde{\tilde{A}}_s$ and $\tilde{\tilde{B}}_s$ have the dimensions of pressure, so

$$\tilde{p}_{ref}\,G_s(v_s) = \tilde{p}_{ref}\,\frac{A_s}{R_{1s}}\exp\left(-R_{1s}\,v_s\right) + \tilde{p}_{ref}\,\frac{B_s}{R_{2s}}\exp\left(-R_{2s}\,v_s\right) \qquad (2.1.10.22)$$

Hence, the dimensionless form of G_s is

$$G_s(v_s) = \frac{A_s}{R_{1s}}\exp\left(-R_{1s}\,v_s\right) + \frac{B_s}{R_{2s}}\exp\left(-R_{2s}\,v_s\right) \qquad (2.1.10.23)$$

2.2 Basic Gas Dynamics Simulations

As may have been mentioned earlier, this document is basically a set of scratch notes based almost entirely on Kapila *et al*.[2] The word "didactic" is just too strong. The ambition of this paper is to, in part, pave the way for writing an "improved" detonation physics computer code cast in three dimensions. The author's present code is really confined to one dimension with the geometric source terms required to access cylindrical and spherical coordinates. A step along the way is to perform gas dynamical simulations for the detonation products. In particular, a shock tube simulation is a viable mime for the detonation problem because the action is driven by a strong moving shock wave followed by an entropic discontinuity. It automatically contains a contact interface propagating at local flow speed between the driver and driven gas columns. In evolving to the detonation problem, the shock wave propels a chemical reaction and a phase transition controlled by the reaction progress variable. This variable acts as a switch within the mixture equation of state that affects a transition from the equation of state for the unreacted explosive to that of the detonation products. So the shock tube acts like a reaction free (or detonation free) detonation problem.

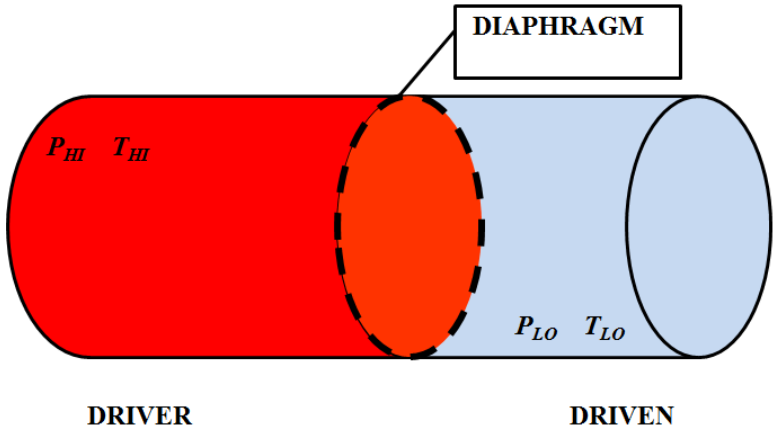

Figure 3. The Shock Tube

2.2.1 The Shock Tube Problem

The field of partial differential equations is replete with a series of canonical problems with attendant, well characterized solutions. For gas dynamics, the shock tube configuration presents a wealth of dynamics for testing numerical algorithms. Otherwise known as the classical Riemann problem, the physical configuration is quite simple, but the fluid dynamics are rather complicated.[7] See Figure 3. The problem is defined in a long tube that is subdivided by an electrically frangible diaphragm. A high pressure gas is placed upstream of the diaphragm on the so-called driver side. Downstream of the diaphragm is the driven side characterized by low pressure gas. In Figure 3, the driver is on the left. When the diaphragm is ruptured, a shock wave radiates into the driven side of the tube at shock speed. The dynamics of the tube are often represented on an *xt*-diagram as shown in Figure 4. Trailing behind the shock wave is a contact wave or interface. This interface is characterized by discontinuities in density and entropy; it propagates at local flow speed. Finally, an expansion wave radiates into the driver section relieving the high pressure. The mathematics of this solution have been examined in great detail by Riemann and many others with exact solutions obtained through Godunov's method.[7]

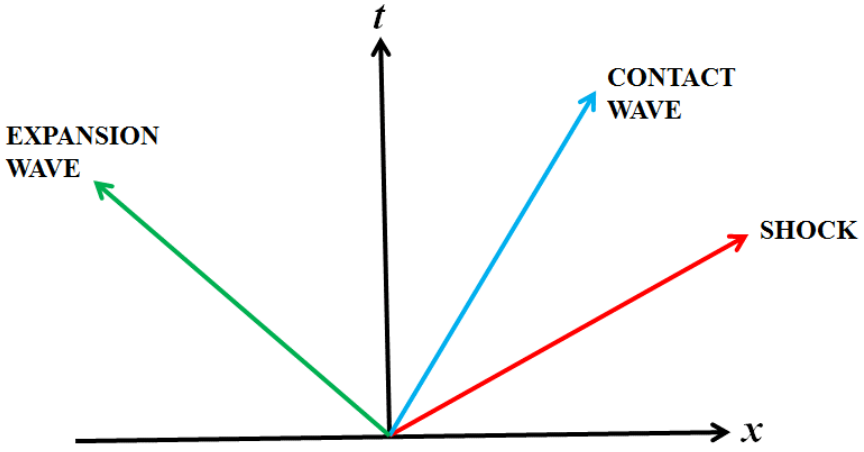

Figure 4. Notional Riemann problem solution on the *xt*-diagram

Due to the workload associated with implementing Godunov's method, an approximate Riemann solver is employed for the purposes of this work. Initial numerical solutions are computed with the use of the Harten-Lax-van Leer (HLL) approximate Riemann solver.[8] This solver is lightweight, efficient and easily adaptable for general equations of state.

2.2.2 The Harten-Lax-van Leer (HLL) Approximate Riemann Solver

In the sincerest interest of brevity, the equations for the HLL solver are not derived here. Still, to highlight the methodology as it differs from say, the Roe scheme [9], the HLL equations are derived from the integral vector form

$$\iint_{x,t} \frac{\partial \vec{U}}{\partial t} + \frac{\partial \vec{F}}{\partial x} dx\, dt \tag{2.2.2.1}$$

In (2.2.2.1), $\vec{U}$ is the vector of conserved variables while $\vec{F}$ is denoted as the flux vector. Although this equation is cast in the Cartesian *x*-coordinate, it is readily adaptable to a coordinate extending across an oblique interface in three-space. Of course, the HLL solution is computed on each side of the hexahedral finite volume cells gridded throughout the flow field. The HLL numerical flux formulas are presented below. For an oblique interface, the vector of conserved variables is written as

$$\vec{U} = \left(\rho, \rho u, \rho v, \rho w, \rho \varepsilon\right)^T \tag{2.2.2.2}$$

The flux vector is expressed as

$$\vec{F} = \left(\rho q, \rho u\, q + p n_x, \rho v\, q + p n_y, \rho w\, q + p n_z, q\left(\rho \varepsilon + p\right)\right)^T \tag{2.2.2.3}$$

where $\hat{n} = \left(n_x, n_y, n_z\right)$ is the unit normal vector at the interface.[10] Both the vector of conserved variables and the flux vector are expressed on the left and right sides of the interface. These upwind quantities are denoted by subscripts *L* and *R*, respectively. Also, the total energy per unit mass is

$$\varepsilon = e + \frac{1}{2}\left(u^2 + v^2 + w^2\right) \tag{2.2.2.4}$$

while the contravariant velocity is denoted as

$$q = u n_x + v n_y + w n_z \tag{2.2.2.5}$$

The HLL solver is constructed by representing dynamics in the *xt*-plane with the use of two waves, a left-traveling wave with speed S_L and a right-traveling wave with speed S_R. The numerical flux is written as follows.

$$\vec{F}^{HLL} = \begin{cases} \vec{F}_L & 0 \le S_L \\ \dfrac{S_R\vec{F}_L - S_L\vec{F}_R + S_L S_R\left(\vec{U}_R - \vec{U}_L\right)}{S_R - S_L} & S_L \le 0 \le S_R \\ \vec{F}_R & S_R \le 0 \end{cases} \tag{2.2.2.6}$$

All of the quantities in (2.2.2.6) are known with the exception of S_L and S_R. These wave speeds require estimation [10], i.e.,

$$S_L = \min\left\{q_L - c_L, \tilde{q} - \tilde{c}\right\}; \quad S_R = \max\left\{q_R + c_R, \tilde{q} + \tilde{c}\right\} \tag{2.2.2.7}$$

where the frozen or generalized speed of sound is denoted as c [11], i.e.,

$$c^2 = \frac{\partial p}{\partial \rho} + \frac{p\,\partial p/\partial e}{\rho^2} \tag{2.2.2.8}$$

Note that the tilde "~" notation in (2.2.2.7) denotes a Roe-averaged quantity.[9] In this case,

$$\tilde{\rho} = \sqrt{\rho_L \rho_R} \tag{2.2.2.9}$$

$$\tilde{u} = \frac{\sqrt{\rho_L}u_L + \sqrt{\rho_R}u_R}{\sqrt{\rho_L} + \sqrt{\rho_L}} \tag{2.2.2.10}$$

$$\tilde{v} = \frac{\sqrt{\rho_L}v_L + \sqrt{\rho_R}v_R}{\sqrt{\rho_L} + \sqrt{\rho_L}} \tag{2.2.2.11}$$

$$\tilde{w} = \frac{\sqrt{\rho_L}w_L + \sqrt{\rho_R}w_R}{\sqrt{\rho_L} + \sqrt{\rho_L}} \tag{2.2.2.12}$$

$$\tilde{q} = \tilde{u}n_x + \tilde{v}n_y + \tilde{w}n_z \tag{2.2.2.13}$$

The Roe-averaged speed of sound must be evaluated from the speed of sound formula, i.e.,

$$\tilde{c}^2 = \frac{\partial \tilde{p}}{\partial \tilde{\rho}} + \frac{\tilde{p}\,\partial \tilde{p}/\partial \tilde{e}}{\tilde{\rho}^2} \tag{2.2.2.14}$$

where

$$\tilde{p} = \tilde{\rho}\left[\tilde{H} - \tilde{e} - \frac{1}{2}\left(\tilde{u}^2 + \tilde{v}^2 + \tilde{w}^2\right)\right] \tag{2.2.2.15}$$

$$\tilde{H} = \frac{\sqrt{\rho_L} H_L + \sqrt{\rho_R} H_R}{\sqrt{\rho_L} + \sqrt{\rho_L}} \tag{2.2.2.16}$$

$$\tilde{e} = \frac{\sqrt{\rho_L} e_L + \sqrt{\rho_R} e_R}{\sqrt{\rho_L} + \sqrt{\rho_L}} \tag{2.2.2.17}$$

Note that H is the total enthalpy per unit mass. With these equations, the first order HLL numerical flux is completely described. For production calculations, total variation diminishing (TVD) methods are employed to formally increase the numerical flux to third order. In this case, extrapolation is applied to the primitive variables (ρ, u, v, w, p, λ) in conjunction with a non-linear limiter to elevate the order of the interface.[12]

3 RESULTS

3.1 Detonation Properties

This section conveys the results of the equations shown in Section 2.1 of this paper for two standard explosives: Livermore Explosive – 17 (LX-17) and Nitromethane (NM).

3.1.1 LX-17

LX-17 is polymer-bonded explosive comprised of 92.5% Triaminotrinitrobenzene (TATB) and 7.5% Kel-F 800. The detonation properties LX-17 are provided in Table 1. Where numerical root estimation is required, the method of False Position is employed with good accuracy.[13] The Hugoniot map including the CJ and von Neumann states is shown in Figure 5. Although a side by side comparison is not presented, there is excellent agreement between the computed values and archived data.

Table 1. Detonation Properties for LX-17

CJ Volume Ratio	0.7597
CJ Specific Volume	3.9879×10^{-4} m^3/kg
Detonation Velocity	7679.947 m/s
CJ Pressure	2.699×10^{10} Pa
CJ Particle Velocity	1845.471 m/s
VN Volume Ratio	0.6900
VN Specific Volume	3.622×10^{-4} m^3/kg
VN Pressure	3.482×10^{10} Pa
VN Particle Velocity	2380.226 m/s

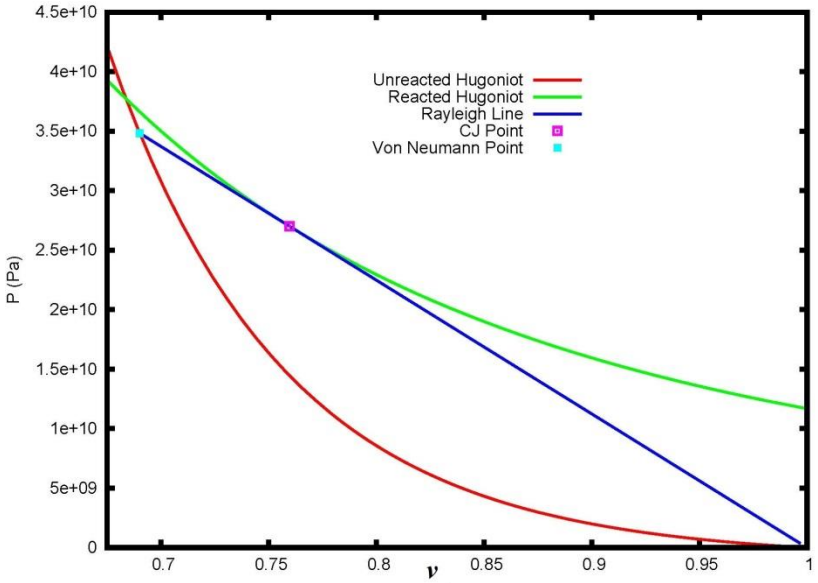

Figure 5. *P-v* Hugoniot map for LX-17 with CJ and von Neumann states

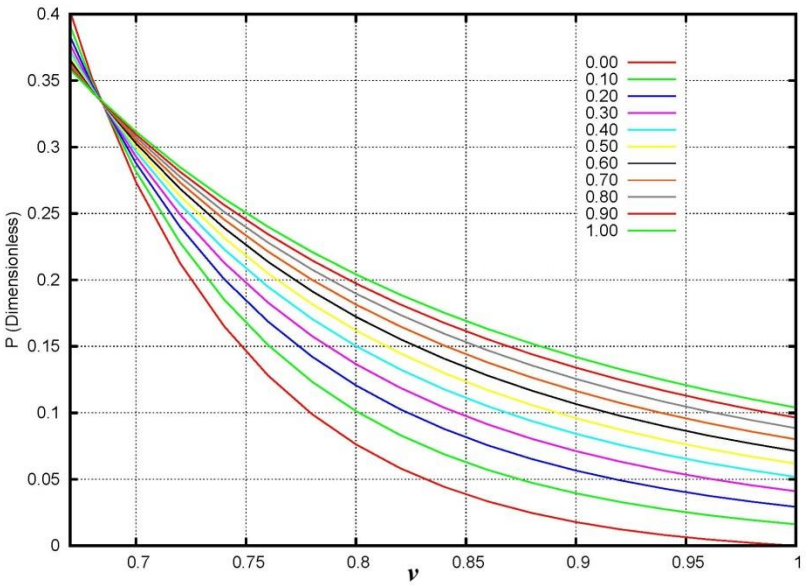

Figure 6. Family of Hugoniots for LX-17 labeled by reaction progress variable λ

Figure 6 contains the family of Hugoniot curves for LX-17 computed for a series of values of the reaction progress variable λ.

3.1.2 Nitromethane

Nitromethane CH_3NO_2 (NM) is a pure CHNO (Carbon-Hydrogen-Nitrogen-Oxygen) explosive of relatively low molecular weight. It is used often in research applications. Its detonation properties are shown in Table 2. Again, root estimation is accomplished via the False Position algorithm. The Hugoniot map for the detonation conditions is presented in Figure 7. CJ and von Neumann states are highlighted. Accordingly, the family of Hugoniots for NM, versus selected values of the reaction progress variable, is shown in Figure 8.

Table 2. Detonation Properties for Nitromethane

CJ Volume Ratio	0.7316
CJ Specific Volume	6.3285×10^{-4} m^3/kg
Detonation Velocity	7038.139 m/s
CJ Pressure	2.099×10^{10} Pa
CJ Particle Velocity	1888.419 m/s
VN Volume Ratio	0.6232
VN Specific Volume	3.944×10^{-4} m^3/kg
VN Pressure	2.948×10^{10} Pa
VN Particle Velocity	2651.478 m/s

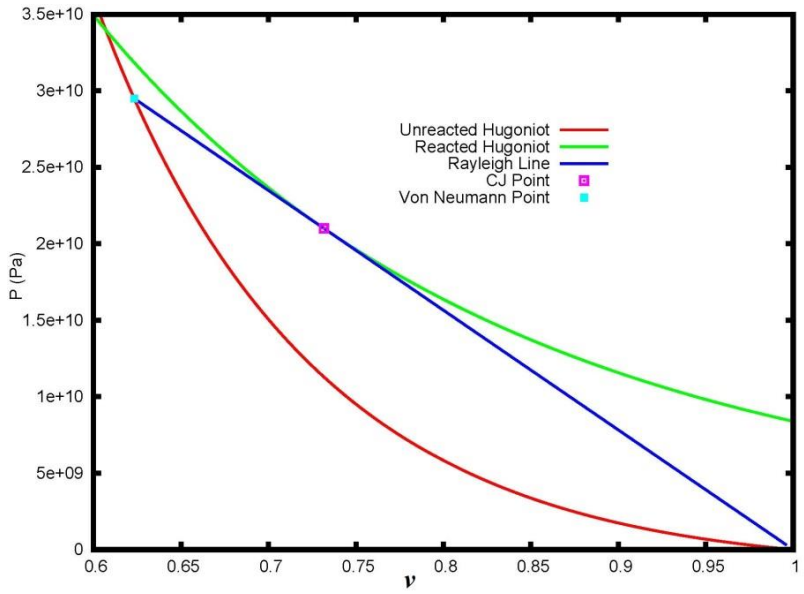

Figure 7. *P-v* Hugoniot map for NM with CJ and von Neumann states

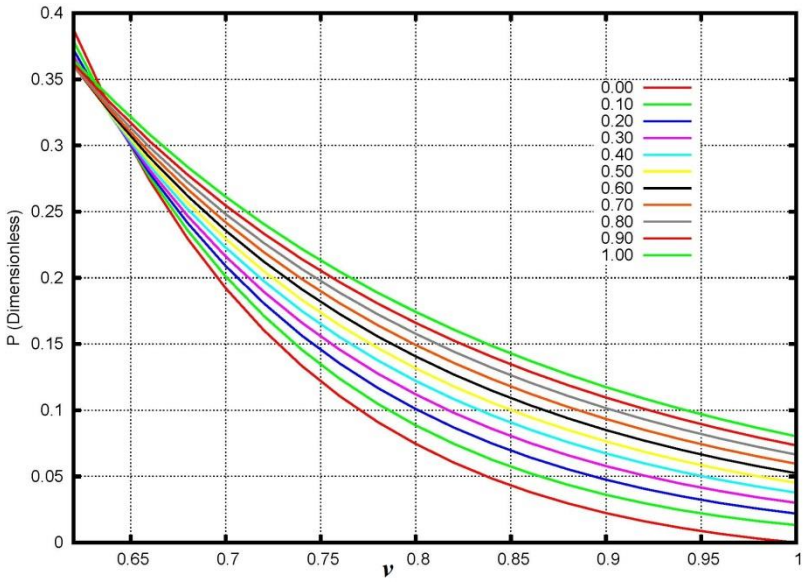

Figure 8. Family of Hugoniots for NM labeled by reaction progress variable λ

3.2 Shock Tube Solutions

An important capability needed for the development of a detonation physics computer program is specific coding segments for calculating properties associated to the JWL equation of state. Shock tube solutions concentrate on gas phase properties whereas a detonation computer code requires properties generated by a mixture equation of state. In the case of the I & G model, the mixture equation of state combines JWL equations of state for both the unreacted explosive and the detonation product gases. This section serves to test the coding segments developed for

the gaseous JWL model. The time integration is accomplished by the second order scheme described in Xu *et al.*[14]

3.2.1 Simulations for LX-17 Vapor

LX-17 is principally comprised of TATB, an aromatic CHNO explosive constructed on the benzene ring. As a result, the catalog of detonation products can be complex. Among these products are compounds such as Nitrogen, Carbon monoxide, Carbon dioxide, water and, of course, Carbon soot. The soot is polymerized or ordered arrays of Carbon atoms resulting from the burn of TATB and some Kel-F. The initial conditions for the LX-17 shock tube are given in Table 3. Note that the specific volume data is calculated for the shock tube with great care because of its more complicated reliance upon the other parameters in the JWL equation of state. The specific volume is identified given pressure and temperature from the solution of (2.1.2.2). For the driver side of the shock tube, this state is illustrated in Figure 9. The points at which the different pressure terms in the JWL can be neglected are indicated. The density, pressure, u velocity and temperature profiles are shown in Figures 10 through 13, respectively. The pressure ratio for the tube is set at 100 to one, not particularly high, but strong enough for illustrative purposes. At the outset of the problem, the contact discontinuity and the main shock wave are captured by the numerical solution, but the contact wave is captured very weakly. This behavior

Table 3. Initial conditions for the LX-17 shock tube problem

Property	Driver Side	Driven Side
Pressure	100 atm	1 atm
Temperature	300 K	300K
Specific Volume	7.771×10^{-3} m^3/kg	7.771×10^{-1} m^3/kg

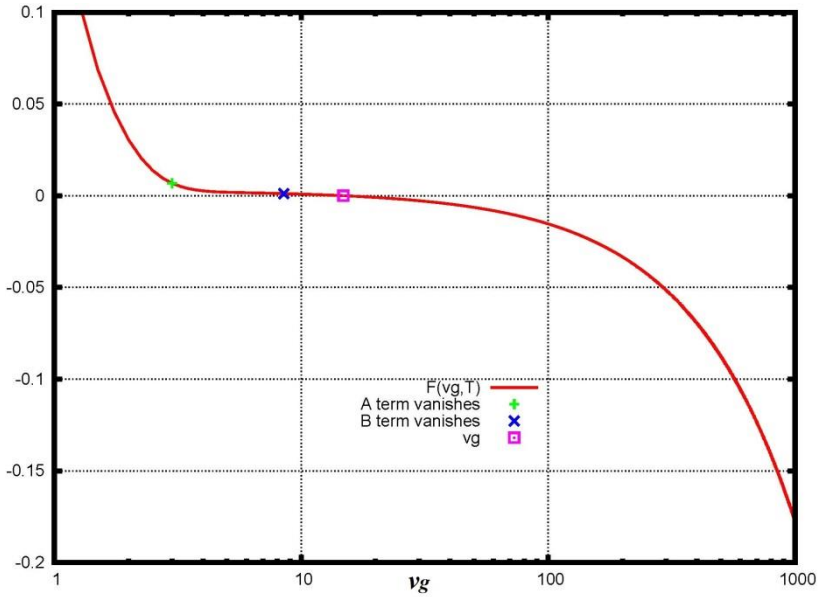

Figure 9. Resolution of the driver side specific volume for LX-17

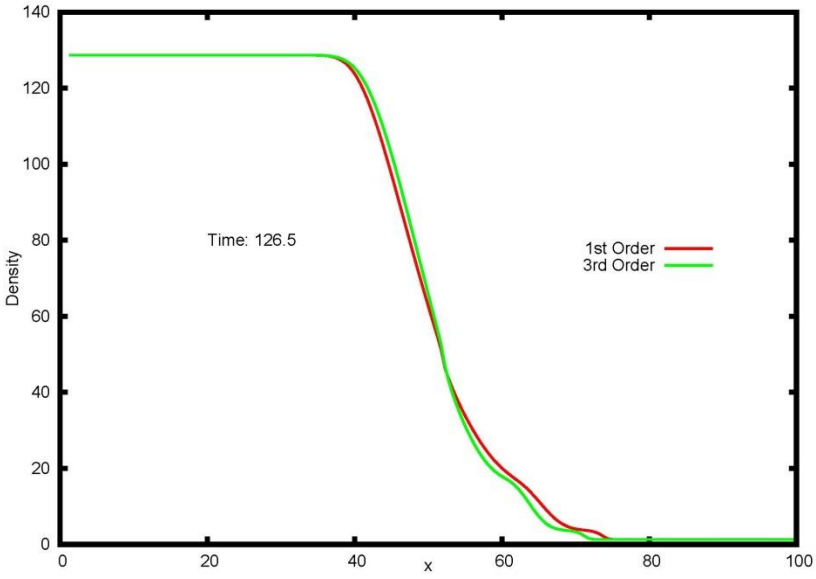

Figure 10. Density profile for the LX-17 shock tube at time 126.5

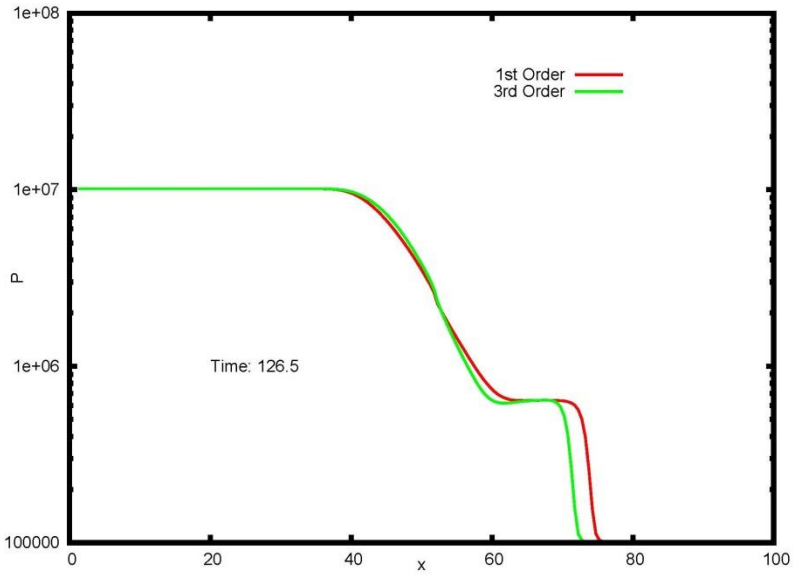

Figure 11. Pressure profile for the LX-17 shock tube at time 126.5

of the solver is due to properties of the HLL shock-capturing scheme. That is, HLL is a non-contact preserving scheme. The changes in the wave front are much more pronounced in Figure 10, the pressure plot. In this case, HLL clearly captures the shock wave. Of course, both the results of both first and third order MUSCL schemes are shown. It is interesting to see the small entropy correction occurring in the rarefaction wave near $x = 50$. One can observe an inflection within the wave form at this location. This inflection occurs in the density, pressure, velocity and temperature plots. It is also evident that the third order solutions are less dissipative than first order solutions because of the MUSCL interpolation. The wave magnitudes are better preserved by the MUSCL interpolation on the set of primitive variables ρ, p, u and T. In the velocity plot, one can also observe the smooth acceleration of the flow field into the rarefaction.

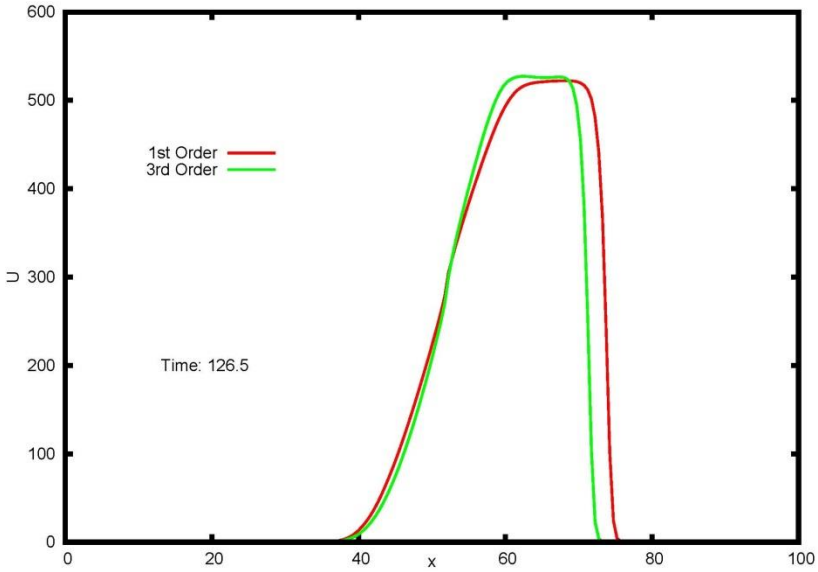

Figure 12. *u*-velocity profile for the LX-17 shock tube at time 126.5

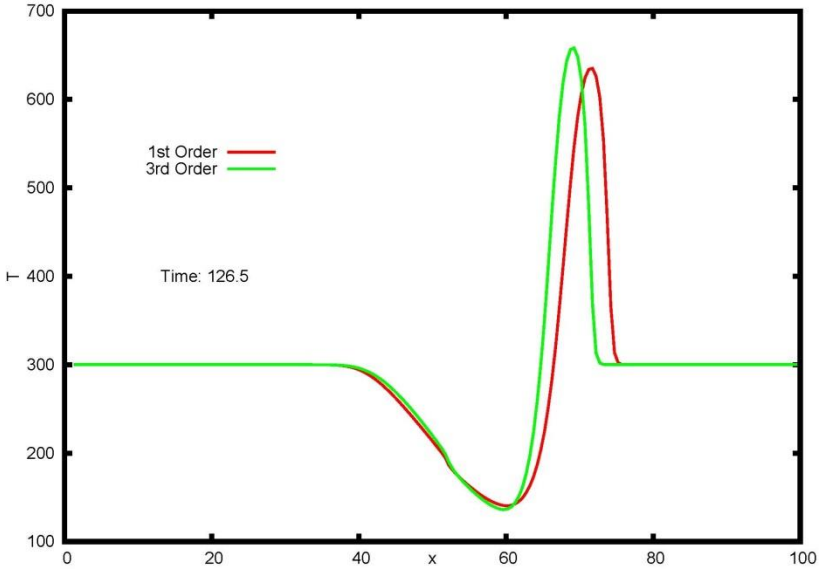

Figure 13. Temperature profile for the LX-17 shock tube at time 126.5

Naturally, HLL is a good test scheme, efficient and easy to program, but for problems where contact is important, one must choose another shock-capturing scheme. In future work, HLLC, the Harten, Lax, van Leer Contact-preserving scheme is our scheme of choice for this application.[15] Still, that effort is cast in the future. The mission at hand is simply to lay the groundwork for a new up-to-date detonation physics computer code that builds upon the limited success of codes gone by and to dole out treacle for the errors and miscues that accompany physics code development.

Based upon insidious personal experience, and as a remedial generality for the HLL solver, all of the input data for the explosive is non-dimensionalized by the detonation conditions (Section 2.1.10). Dimensions are reapplied to the data just prior to output. In this way, the solver

operates strictly on dimensionless quantities. This has the altogether desirable effect of compacting the ranges of variation of various physical properties. The solver is less likely to suffer some pathology resulting from an extreme condition say, a lack of convexity or some wild spike in pressure.

3.2.2 Simulations for Nitromethane Vapor

In some sense, the simulation of NM detonation products is less interesting than those for LX-17. Why? NM is substantially simpler in composition and takes the form of polar liquid solvent at room temperature. It has many industrial applications aside from being a liquid explosive often used in testing. If purified with no contaminants, it is a true CHNO explosive. The shock tube initial conditions for NM are given in Table 4 whereas Figure 14 illustrates the specific volume attained on the driver side of the shock tube. Note that in this case, the initial driver specific volume falls in between the two main JWL pressure terms. The density, pressure, velocity and temperature profiles for the NM shock tube are provided in Figures 15 through 18,

Table 4. Initial conditions for the NM shock tube problem

Property	Driver Side	Driven Side
Pressure	100 atm	1 atm
Temperature	300 K	300 K
Specific Volume	5.8933×10^{-3} m^3/kg	5.621×10^{-1} m^3/kg

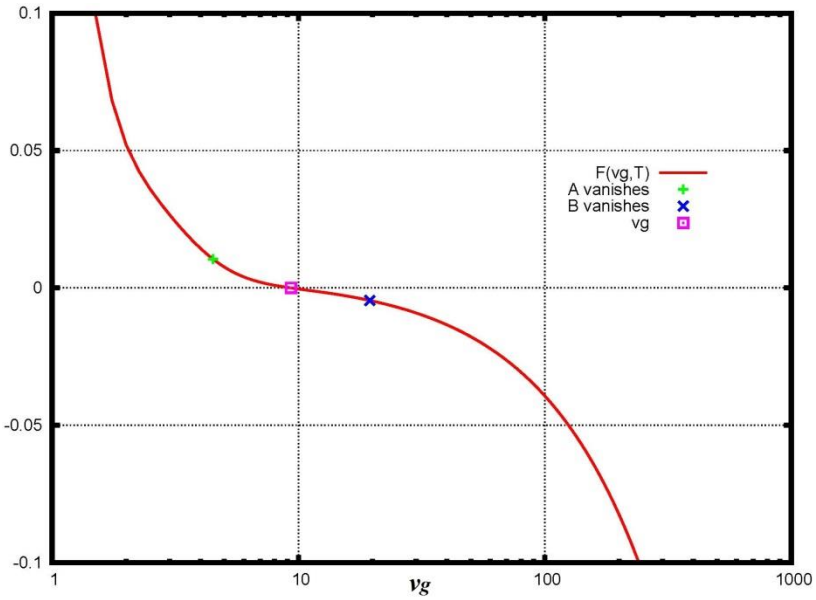

Figure 14. Resolution of the driver side specific volume for NM

respectively. There is a great deal of similarity between the shock tube solutions for LX-17 and NM, and well there should be since the initial conditions are virtually the same. Still, the process of dimensionless scaling helps map the numerical solutions for the detonation products of different explosives onto the same physical properties space. As one may observe, there is a

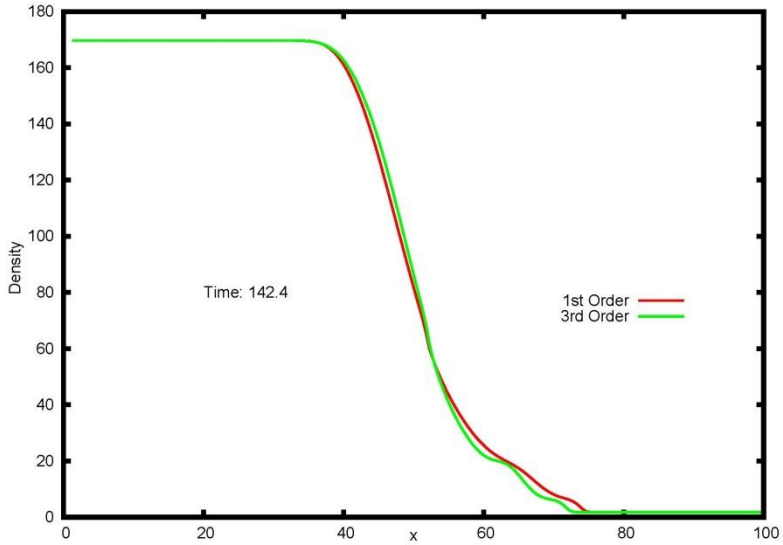

Figure 15. Density profile for the NM shock tube at time 142.4

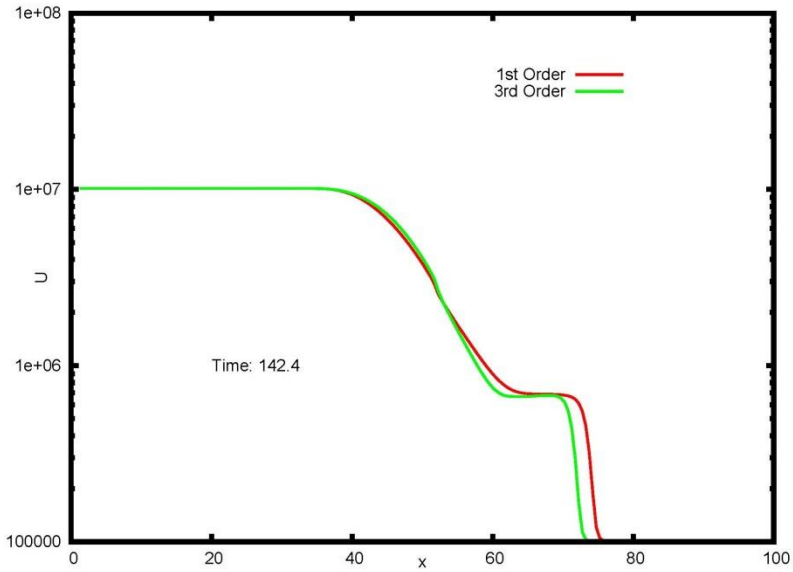

Figure 16. Pressure profile for the NM shock tube at time 142.4

great deal of similarity between the shock tube solutions for LX-17 and NM detonation products.

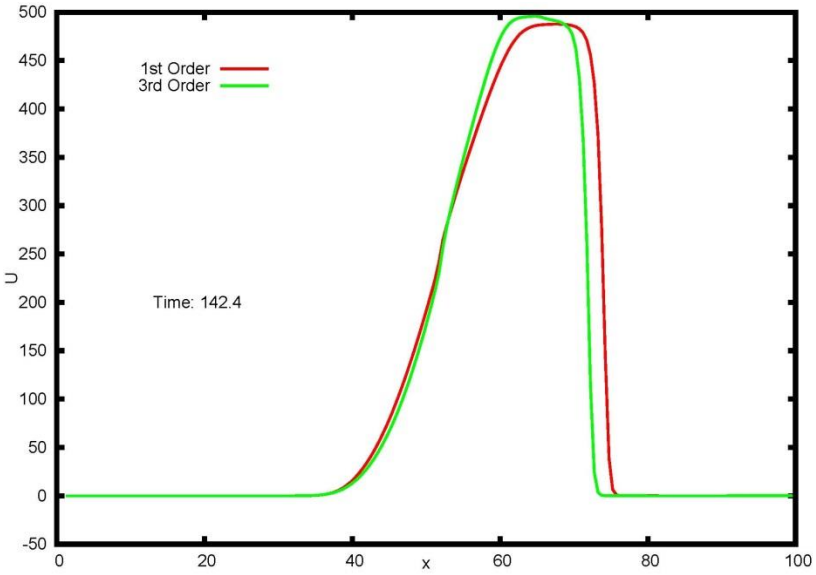

Figure 17. *u*-velocity profile for the NM shock tube at time 142.4

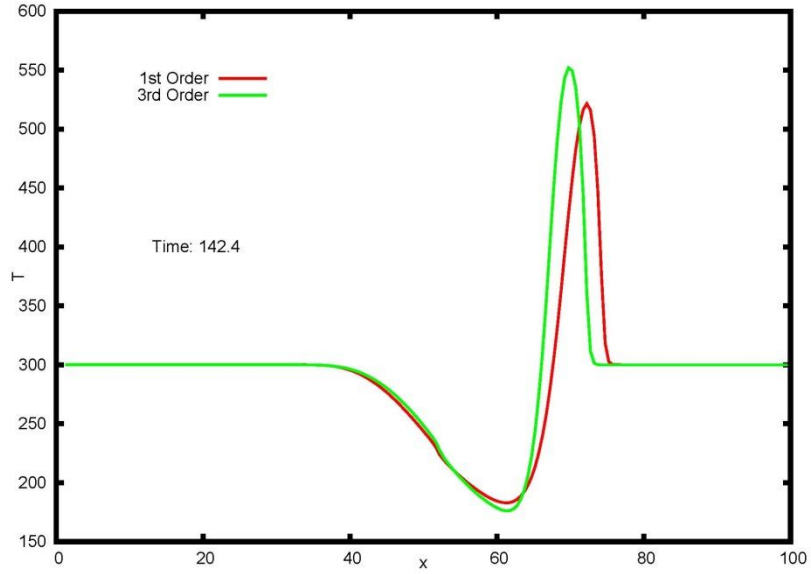

Figure 18. Temperature profile for the NM shock tube at time 142.4

4 CONCLUSIONS AND RECOMMENDATIONS

This paper is, by intent, rather mechanical and incomplete. None of the technical topics within are taken to an end conclusion or wrapped up. Instead, this write-up is intended to be more like a chalk board where a series of disparate notes and derivations are recorded. At least in the view of the author, each of the technical issues brought onto the floor are important structures needed in the development of a detonation physics computer program. My claim is that one must have a working knowledge of the equations of state for the solid explosive and for the detonation products prior to performing a successful numerical simulation of the detonation of a condensed explosive. The system of equations of state, including the reaction rate expression, must be completely self-consistent because the detonation state is defined by these equations through the Hugoniot relations.

Here, we have followed the work of Kapila *et al.* to characterize the steady state detonation conditions for LX-17 and for NM. All of the principal detonation properties can be elucidated by examining the I & G equation of state, along with the flow equations in one dimension. Only basic numerical techniques such as root finding are required to accurately determine the properties of the detonation. Moreover, the Hugoniot plot, the CJ and VN states are easily extracted from the equations. Also, mixture Hugoniots are generated for a selection of values of the reaction progress variable. Along the way, we have elucidated techniques for extracting different explosive properties from the equation of state.

As a final step, the Harten-Lax-van Leer shock-capturing scheme has been applied to solve the shock tube or Riemann problem for the I & G detonation products, in particular, for the JWL equation of state. Example calculations are shown for LX-17 and NM, including the computation of the frozen speed of sound. Although the problems are cast in one dimension, numerical flux formulas are cast in three dimensions to promote generality. Both the first order interface and the third order interface (produced by MUSCL interpolation formulas with appropriate non-linear limiters) are tested for the shock tube.

Following the scattering of ideas discussed earlier, there are a set of next logical steps needed to develop a detonation physics computer program. First, the traverse numerical flux formulas require installation and testing. This operation is orderly since only indices and unit vector components require changes. As a second step, it is necessary to incorporate contact through coding the HLLC flux formulas. Doing so increases the accuracy of the contact interface, but the algorithm is more complex and must be carefully coded. Finally, the reaction progress equation is to be coupled into the mixture equation of state, and a series of one, two and three-dimensional detonation physics problems are to be solved by using the new computer program. The solutions are to be compared with archival data. Then the code is to be tested for other explosives such as Trinitrotoluene (TNT). When satisfactory performance is exhibited by the computer program, then a porous explosive model is to be implemented.

REFERENCES

1. Tarver, C.M., Hallquist, J.O. and Erickson, L.M., "Modeling short pulse duration shock initiation of solid explosives", *Eighth International Symposium on Detonation*. Albuquerque, NM, 1985.

2. Kapila, A.K., Schwendeman, D.W., Bdzil, J.B. and Henshaw, W.D., "A study of detonation diffraction in the ignition-and-growth model", *Combustion Theory and Modeling*, Vol. 11, No. 5, pp. 781-822, 2007.

3. Menikoff, R., "Complete Mie-Grüneisen Equation of State", Technical Report, LA-UR-12-22592, Los Alamos National Laboratory, 2016.

4. Zukas, J.A. and Walters, W.P., Eds., *Explosive Effects and Applications.* Springer, New York, New York, 1998.

5. Cooper, P., *Explosives Engineering.* Wiley-VCH, New York, New York, 1996.

6. von Neumann, J., "Theory of Detonation Waves", OSRD 549, Institute for Advanced Study, Princeton, New Jersey, 1942.

7. Toro, E.F., *Riemann Solvers and Numerical Methods for Fluid Dynamics - A Practical Introduction,* 3rd Ed. Springer, New York, New York, 2009.

8. Harten, A., Lax, P.D. and van Leer, B., "On upstream differencing and Godunov-type schemes for hyperbolic conservation laws", *SIAM Review*, Vol. 25, No.1, pp. 35-61, 1983.

9. Glaister, P., "An approximate linearised Riemann solver for the Euler equations for real gases", *Journal of Computational Physics*, Vol. 74, pp. 382-408, 1988.

10. Batten, P., Clarke, N., Lambert, C. and Causon, D.M., "On the choice of wavespeeds for the HLLC Riemann solver", *SIAM Journal of Scientific Computing*, Vol. 18., No. 6, pp. 1553-1570, 1997.

11. Nance, D.V., "Roe's Method for Real Gas Mixtures", Technical Report, AFRL-RW-EG-TR-2014-051, Munitions Directorate, Air Force Research Laboratory, 2014.

12. Hirsch, C., *Numerical Computation of Internal and External Flows, Vol. 2, Computational Methods for Inviscid and Viscous Flows.* John Wiley & Sons, new York, New York, 1990.

13. Dahlquist, G. and Björck, A., *Numerical Methods.* Prentice-Hall, Englewood Cliffs, New Jersey, 1974.

14. Xu, S., Aslam, T. and Stewart, D.S., “High resolution numerical simulation of ideal and non-ideal compressible reacting flows with embedded internal boundaries”, *Combustion Theory and Modeling,* Vol. 1, pp. 113-142, 1997.

15. Toro, E.F., Spruce, M. and Speares, W., “Restoration of the contact surface in the HLL-Riemann solver”, *Shock Waves,* Vol. 4, pp. 25-34, 1994.

DISTRIBUTION LIST

AFRL-RW-EG-TR-2019-087

*Defense Technical Info Center
8725 John J. Kingman Rd Ste 0944
Fort Belvoir VA 22060-6218

AFRL/RWML (1)
AFRL/RWORR (STINFO Office) (1)